SYNTHESIS OF DUAL-PURPOSE RESINS FOR SORPTION OF TOXIC METAL IONS AND ORGANIC CONTAMINANTS

BY

IHSAN BUDI RACHMAN

A Thesis Presented to the

DEANSHIP OF GRADUATE STUDIES

KING FAHD UNIVERSITY OF PETROLEUM & MINERALS

DHAHRAN, SAUDI ARABIA

In Partial Fulfillment of the
Requirements for the Degree of

MASTER OF SCIENCE

In

CHEMISTRY

MAY, 2017

KING FAHD UNIVERSITY OF PETROLEUM & MINERALS

DHAHRAN- 31261, SAUDI ARABIA

DEANSHIP OF GRADUATE STUDIES

This thesis, written by **IHSAN BUDI RACHMAN** under the direction his thesis advisor and approved by his thesis committee, has been presented and accepted by the Dean of Graduate Studies, in partial fulfillment of the requirements for the degree of **MASTER OF SCIENCE IN CHEMISTRY**.

Dr. Tawfik Abdo Saleh
(Advisor)

26/9/2017
Dr. Abdulaziz A. Al-Saadi
Department Chairman

Sk. Asrof Ali
Prof. Shaikh Asrof Ali
(Member)

Prof. Salam A. Zummo
Dean of Graduate Studies

2/10/17
Date

Dr. Jameel Raddah Al Thagfi
(Member)

This Thesis is dedicated to my father -may Allah grant him Jannat-, my family, friends, chemistry world and my lovely wife.

ACKNOWLEDGMENTS

Alhamdulillah, with gratitude to Almighty Allah who had made it possible for me to complete this study successfully. I would like to thank The King Fahd University of Petroleum and Minerals (KFUPM) for the scholarship and opportunity to study at master program of Chemistry Department.

Foremost, I wish to register my profound gratitude appreciation to my thesis advisor Dr. Tawfik Abdo Saleh. He was supportive supervisor since the day of advisor selection. I have gotten so much laboratory skills, knowledge and to manage it for this thesis. My special thanks also to committee member of my thesis committee, Prof. Shaikh Asrof Ali and Dr. Jameel Raddah Al Thagfi for their valuable suggestion and contribution towards the success of this work.

Beside that, thank to the chairman of Chemistry Department Dr. Abdulaziz A. Al-Saadi for his assistance and numerous help. My appreciation also to all faculty members who teach me during study in chemistry KFUPM, Dr. Fettouhi, Dr. Chanbahsa, Dr. Al-Imam, Dr. Mazumder, Dr. Kawde, Prof. Wazeer and Prof. Badawi. Also to technicians and staff of department, especially Mr. Darwin for their support and assistance.

I would like to thank labmates, Cheche, Onawole, Akram, Islam, Saddam and Alaaldin for the discussion, kindness, and encouragement during of my research.

Special thanks to all Indonesian community in KFUPM, my family member, most especially my wife, Noerma Madjid Riyadi for their love and patience throughout the M.Sc program. All of this remain nothing without full support from my family. Thank you for all your encouragement.

TABLE OF CONTENTS

LIST OF TABLES

LIST OF FIGURES

LIST OF ABBREVIATIONS

AIBN	:	2,2′-Azoisobutyronitrile
BET	:	Brunauer-Emmett-Teller
BJH	:	Barrett-Joyner-Halenda
CCD	:	central composite design
DMSO	:	Dimethylsulfoxide
DSC	:	differential scanning calorimetry
EDX	:	Energy-dispersive X-ray spectroscopy
FT-IR	:	Fourier Transform Infrared
HCDAPE	:	hydrophobic cross-linked dianionic polyelectrolyte
HCPZA	:	hydrophobic cross-linked polyzwitterionic acid
ICP-MS	:	Inductively Coupled Plasma – Mass Spectrometer
MB	:	Methylene Blue
NMR	:	Nuclear Magnetic Resonance
RSM	:	response surface method
SEM	:	Scanning Electron Microscope
TGA	:	Thermogravimetric analysis
TMS	:	Tetramethylsilane
UV-vis	:	Ultra Violet – Visual
XPS	:	X-ray Photoelectron Spectrometer

ABSTRACT

Full Name : Ihsan Budi Rachman

Thesis Title : Synthesis Of Dual-Purpose Resins For Sorption Of Toxic Metal Ions And Organic Contaminants

Major Field : Chemistry

Date of Degree : May 2017

A new highly efficient cross-linked polymers were synthesized via cyclotetrapolymerization of hydrophilic [(diallylamino)propyl]phosphonic acid hydrochloride (72 mol%), hydrophobic *N*,*N*-diallyl-1-[6-(biphenyl-4-yloxy)hexylammonium chloride (18 mol%), cross-linker 1,1,4,4-tetraallylpiperazinium dichloride (10 mol%) with an equivalent amount of alternating SO_2 units (100 mol%). The pH-responsive resin chemically tailored with the aminopropylphosphonate chelating ligand and hydrophobic chain of $(CH_2)_6OC_6H_4$-C_6H_5 is designed to capture toxic metal ions and organic contaminants simultaneously. The developed resin was used for the remediation of Hg(II) ions and methylene blue from aqueous solutions as models. The experimental conditions were optimized under response surface methodology as an environmentally friendly method. The adsorption efficiency for Hg(II) was ≈100% at 10 ppm initial concentration at pH 5 at 25 °C, while it was 80% for removal of the dye in a single pollutant system. Interestingly, the resin demonstrated its remarkable efficacy in simultaneous and complete removal of Hg(II) and the dye from their mixture. Increased removal of the dye (≈100 %) in the presence of Hg(II) was attributed to the synergistic effect. The equilibrium data were evaluated by Langmuir and Freundlich isotherm models. By using 1.0 M HCl solution, the adsorbed Hg(II) ions were desorbed at high effectiveness and the methylene blue was recovered with acetone. Another polymer was also synthesized and tested for Cr(III) removal.

ملخص الرسالة

الاسم الكامل : إحسان بودي راشمان

عنوان الرسالة : تحضير راتنجات ثنائية الغرض لاستخلاص أيونات المعادن السامة والملوثات العضوية

التخصص : كيمياء

تاريخ الدرجة العلمية : مايو ٢٠١٧

تم تحضير بوليمر جديد عالي الكفاءة من النوع المشبك عن طريق بلمرة [(diallylamino)propyl]phosphonic acid hydrochloride النافرة للماء ب (72 مول %)، *N*,*N*-diallyl-1-[6-(biphenyl-4-yloxy)hexylammonium chloride النافرة للماء ب (18 مول %)، 1,1,4,4-tetraallylpiperazinium dichloride من النوع المشبك ب(10 مول %) مع كمية مماثلة من ثاني أكسيد الكبريت (100 مول %). تمت المعالجة الكيميائية لراتنج الاستجابة للرقم الهيدروجيني مع رابطة aminopropylphosphonate وسلسة نافرة للماء من $(CH_2)_6OC_6H_4$-C_6H_5 والتي صممت لتقوم باصطياد أيونات المعادن السامة والملوثات العضوية في آن واحد. استُخدِم الراتنج الذي تم تطويره لمعالجة المحاليل المائية كنموذج والتي تحتوي على أيونات الزئبق والميثيلين الأزرق. تم تحسين الظروف التجريبية باستخدام طريقة سطح الاستجابة والتي تعتبر طريقة صديقة للبيئة. كفاءة الامتزاز للزئبق كانت ≈ 100 % عند تركيز مبدئي 10 جزء من المليون ورقم هيدروجيني 5 ودرجة حرارة 25 درجة مئوية. بينما كانت النتيجة 80 % بالنسبة لإزالة الصبغة في نظام ذو ملوث واحد. المثير للاهتمام هو أن الراتنج أعطى نتائج ملحوظة في الإزالة الكاملة لكل من الزئبق والصبغة في آن واحد من الخليط. الزيادة الملحوظة في إزالة الصبغة ≈ 100 % في تواجد الزئبق يعود إلى تأثير التآزر. تم حساب بيانات التوازن باستخدام نماذج لانجماير وفرندلج. باستخدام 1 مولارتي من محلول حمض الهيدروكلوريك أيونات الزئبق الذي تم امتزازها تم استردادها بكفاءة عالية، كما تم استرجاع الميثيلين الأزرق باستخدام الاسيتون. كم تم تحضير بوليمر آخر وتم اختباره لإزالة أيونات الكروم.

CHAPTER 1

INTRODUCTION

Introduction of foreign matters into the water as a result of various activities (natural and anthropogenic) has led to the deterioration of quality of water making it unsuitable for desired purposes. One of such foreign matters are the heavy metals, which poses a serious health problems to humans as wells as other flora and faunas in the environment [1]. Sustainable water supplies are vital for agriculture, industry, energy production, and domestic consumption. However, in a classic case of unintended consequences, heavy metals are being added to environment and is now considered as a significant risks to groundwater and drinking water sources [2]. Recently, more stringent regulations for drinking water quality are being recommended to be implemented [3].

Heavy Metal is any metal or metalloid of environmental concern and considered to be having toxic effect even at a very low concentration. The major elements in this category includes arsenic (As), cadmium (Cd), chromium (Cr), copper (Cu), lead (Pb), mercury (Hg), nickel (Ni), cobalt (Co) and zinc (Zn). They are found normally below the earth's crust in nature and are non-biodegradable. Heavy metals are pollutants usually encountered in soil and water [4]. Some of these metals are essential in low amount in humans and other animals and only be toxic or poisonous when their concentration is high. Bioaccumulation of heavy metals in the biotic system is the major health hazard attributed to them. Several industrial activities such as chemical manufacturing, electroplating, tannery, painting, mining, metallurgy, nuclear and other industries are the major contributors of heavy metals into the environment [5]. Considering the health impacts associated with heavy metals

exposure identified in the Drinking Water Advisory of the United States Environmental Protection Agency, more and more stringent regulations have been modified periodically to make sure that discharge from the above mentioned activities are well treated before finally released into the environment [6].

Besides heavy metal ions, another pollutant is dyes contaminant. There was many industries released dyes pollutant: polymer plastics for packaging and domestic uses, synthetic leather, textile for clothes, paper, food and beverage, pigment, inks, adhesive materials, etc. It produced a lot of colored water to surrounding. Dyes from industry mostly came from artificial dyes because less cost, massive production, long live time than natural dyes, and many colour could be produced through syhetesis methods. More than 100,000 kind of dyes available to use and estimated 1×10^6 dyestuff made every year. Contaminated water could be seen based on it appearances even at very low concentration of dyes.

With the extensive industrialization and urbanization going on in the country, the quality of limited groundwater resources is being endangered by chemical pollution especially from heavy metals. Contamination of water supplies from industrial waste is as a result of various types of industrial processes and disposal practices. Industries that use large volumes of water for processing have the potential to pollute waterways through discharge of their waste into streams and rivers, runoffs and seepages of stored waste into nearby water sources. Considering the health impacts associated with heavy metals exposure, there is a much greater need to remove these toxic metals from water and protect the water resources from deteriorating in quality. Since it is strongly recommended that pollutants should be removed from wastewater with high efficiency before discharge into the environment, different remediation technologies are being applied for water treatment such as

electrocoagulation, membrane filtration, ion exchange, etc.; each have recorded varying levels of success and inherent limitations.

In the country which is faced with shortage of freshwater resources, it is imperative that water is kept free from pollution in order to partly ease the effects of water scarcity. With the extensive industrialization drive being pursued in the country, the quality of limited groundwater resources as well as surface water are threatened by pollution from various toxic pollutants as a result of high industrialization, urbanization and other anthropogenic activities. Considering the health impacts associated with heavy metals exposure identified in the Drinking Water Advisory of the United States Environmental Protection Agency [6], there is a need to develop techniques which are environmentally friendly, simple-to-use, effective and efficient in removing pollutants from water. Adsorption using polymer materials as adsorbent is regarded as one of the most effective methods to remove pollutants from wastewaters. This creates the opportunity for further research in exploring the structural properties of various synthetic materials in the removal of toxic metals and organic pollutants in water resource.

1.1 Methodology

1.1.1 Synthesis of Resin Polymer

2,2′-Azoisobutyronitrile (AIBN), purchased from Fluka AG, was purified by crystallizing from a chloroform-ethanol mixture. Dimethylsulfoxide (DMSO) was purified by drying (CaH_2) and distilling at 64-65°C (4 mmHg). *p*-Phenylphenol (**1**), 1,6-dibromohexane (**2**) and diallylamine (**4**) were purchased from Fluka AG. Cross-linker **8** was synthesized using

a literature procedure [16]. Monomer **7** [17] and 4-(6-Bromohexyloxy)biphenyl (**3**) [18] were prepared as described.

1.1.2 Characterization of Resin Polymer

Perkin Elmer 2400 Series II CHNS/O Elemental Analyzer was used for the elemental analysis. Perkin Elmer Elemental Analyzer Series 11 Model 2400 (Waltham, Massachusetts, USA) was used for elemental analysis.

IR analyses were performed on a Thermo scientific FTIR spectrometer (Nicolet 6700, Thermo Electron Corporation, Madison, WI, USA).

NMR spectra were obtained in a JEOL LA 500 MHz spectrometers using $CDCl_3$ with tetramethylsilane (TMS) as internal standard (^1H signal at δ 0 ppm), while taking HOD signal at δ4.65 ppm and dioxane signal at 67.4 ppm as internal and external standards, respectively.

Solid-state CP MAS ^{13}C NMR spectrum was recorded on a Bruker 400 MHz NMR Spectrometer using spin rate of 4000 Hz using a chemical shift of CH_2 of adamentane at 29.5 ppm as an external standard.

Scanning electron microscope (SEM) was used to examine the morphology of the polymer surface before and after the adsorption of Hg(II). Energy-dispersive X-ray spectroscopy (EDX) fitted with a detector model X-Max was used to obtain the elemental spectrum and get elemental analyses of the original polymer and pollutant-loaded polymer.

Thermogravimetric analysis (TGA) using an SDT Q600 thermal analyzer from TA instruments, USA, was conducted to evaluate the thermal stability of the prepared polymer.

The temperature was raised at a constant rate of 10°C/min over a temperature range of 20–800°C in an air atmosphere flowing at a rate of 100 mL/min.

The specific surface area and pore size distribution were determined by the methods of Brunauer-Emmett-Teller (BET) and Barrett-Joyner-Halenda (BJH). Mercury analyzer was employed to monitor the concentfration of Hg(II). The concentration of the tested dye was monitored using UV-vis spectrophotometer using optical quartz cuvettes.

1.2 Objective of Research

The main objectives of this research are:

1. To synthesize polymers of binary nature; hydrophobic and hydrophilic nature properties.
2. To demonstrate efficiency of the prepared materials for sorption of toxic metals and organic contaminants
3. To optimize the treatment conditions such as pH, material dosage, temperature, contact time, initial concentration of heavy metal and dyes pollutant and agitation rate.
4. Test the removal capacity of heavy metals and dyes poluutant by the synthesised polymers from real wastewater under the optimum treatment conditions.

CHAPTER 2

TAILORING HYDROPHOBIC AND ACTIVE SITES IN POLYZWITTERIONIC RESIN FOR SIMULTANEOUS CAPTURING OF HG(II) AND METHYLENE BLUE: OPTIMIZATION USING RESPONSE SURFACE METHOD

2.1 Introduction

Heavy metal ions are non-biodegradable pollutants which are accumulated in groundwater and on the soil surface as a waste of some industrial processes such as minerals mining, pigments for color enhancement, and anti-corrosion additive materials coating. Heavy metal ions over the normal limit can be toxic that may cause a variety of diseases, including loss of memory, kidney and renal problems, diarrhea, lung damage, cancer, as well as reproductive disorders. Mercury is the most dangerous metal ion due to its toxicity [1, 2].

Other types of pollutants are the organic compounds having adverse effects on the environment. Dyes are massively used in industry such as textile, paper painting, leather, plastics, rubber and dying [3, 4]. Dyes redemption from textile industry leads to serious environmental damages owing to their difficult degradability. 3,7-bis(dimethylamino)phenothiazine-5-ium-chloride or methylene blue (MB) is one example from many dyes used extensively in industry; it can be absorbed by plants, furthermore consumed by humans and accumulated in humans tissue and cause many diseases in humans owing to its non-biodegradability and toxicity.

To minimize the impact on the environment, there are many methods for the removal of pollutants, like membrane processes, continuous liquid-solid separation, liquid extraction, ion exchange, filtration, electrolytic recovery, reverse osmosis, advanced oxidation processes adsorption, and chemical precipitation as sulfides, hydroxides or carbonates and adsorption with ultrasonically assisted acid treatment [5]. Among these, adsorption methods achieved considerable significance because of their efficiency, simplicity, low cost, usefulness at low concentrations. Until now, numerous publications dealt with the removal of single pollutant, while few studies have been reported for simultaneous removal of organic and metal pollutants by adsorption techniques [6, 7].

Choosing an appropriate and good adsorbent material for specific pollutant target should be the first priority for a successful adsorption process. Conventional adsorbent like clay activated carbon, and nanomaterials are usually used for heavy metal ions and dyes removal from wastewater [8]. Non-toxic, biodegradable and eco-friendly natural polymers such as cellulose, chitosan, and starch are also used because of their natural abundance, high efficiency and low cost, [9]. At industrial applications, there is a need for more advanced properties of an adsorbent such as fast adsorption kinetics, high capacity, and temperature stability [10-15]. Polymeric materials could be tailored with judicious designing that can fulfill the industrial requirement.

The current work describes the synthesis of a novel functionalized resin embedded with the residues of the chelating ligand of aminopropyl phosphonate and hydrophobic pendants (**Figures 2.1 and 2.2**). The resin could be used as a sorbent for simultaneous removal of Hg(II) ions and methylene blue from aqueous solution.

2.2 Experimental

2.2.1 Material

2,2′-Azoisobutyronitrile (AIBN), purchased from Fluka AG, was purified by crystallizing from a chloroform-ethanol mixture. Dimethylsulfoxide (DMSO) was purified by drying (CaH_2) and distilling at 64-65°C (4 mmHg). *p*-Phenylphenol (**1**), 1,6-dibromohexane (**2**) and diallylamine (**4**) were purchased from Fluka AG. Cross-linker **8** was synthesized using a literature procedure [16]. Monomer **7** [17] and 4-(6-Bromohexyloxy)biphenyl (**3**) [18] were prepared as described.

$Hg(NO_3)_2$ standard solution (1000 ppm) was used to prepare the diluted solutions of the required concentrations. Sodium hydroxide and nitric acid were purchased from Sigma–Aldrich. Millipore water (18.2 MΩ·cm) was used for the adsorption study. Reagent grade organic solvents were used.

2.2.2 Characterization Techniques and procedures

Perkin Elmer 2400 Series II CHNS/O Elemental Analyzer was used for the elemental analysis. Perkin Elmer Elemental Analyzer Series 11 Model 2400 (Waltham, Massachusetts, USA) was used for elemental analysis, while IR analyses were performed on a Thermo scientific FTIR spectrometer (Nicolet 6700, Thermo Electron Corporation, Madison, WI, USA). NMR spectra were obtained in a JEOL LA 500 MHz spectrometers using $CDCl_3$ with tetramethylsilane (TMS) as internal standard (^1H signal at δ 0 ppm), while taking HOD signal at δ4.65 ppm and dioxane signal at 67.4 ppm as internal and external standards, respectively. Solid-state CP MAS ^{13}C NMR spectrum was recorded on

a Bruker 400 MHz NMR Spectrometer using spin rate of 4000 Hz using a chemical shift of CH_2 of adamentane at 29.5 ppm as an external standard.

Scanning electron microscope (SEM) was used to examine the morphology of the polymer surface before and after the adsorption of Hg(II). Energy-dispersive X-ray spectroscopy (EDX) fitted with a detector model X-Max was used to obtain the elemental spectrum and get elemental analyses of the original polymer and pollutant-loaded polymer. Thermogravimetric analysis (TGA) using an SDT Q600 thermal analyzer from TA instruments, USA, was conducted to evaluate the thermal stability of the prepared polymer. The temperature was raised at a constant rate of 10°C/min over a temperature range of 20–800°C in an air atmosphere flowing at a rate of 100 mL/min. The specific surface area and pore size distribution were determined by the methods of Brunauer-Emmett-Teller (BET) and Barrett-Joyner-Halenda (BJH). Mercury analyzer was employed to monitor the concentration of Hg(II). The concentration of the tested dye was monitored using UV-vis spectrophotometer using optical quartz cuvettes.

2.2.3 Synthesis of monomer precursor 5

A solution of bromide **3** (4.60 g, 13.8 mmol) and diallylamine **4** (6.7 g, 69 mmol) in toluene (6 mL) was heated under N_2 at 100 °C for 24 h. The reaction mixture was taken in water 20 (mL) containing NaOH (0.60 g, 15 mmol) and extracted with ether (2×25 mL). The organic extract was dried (Na_2SO_4) and concentrated. The residual liquid was purified by chromatography over silica gel using ether/hexane mixture as eluent to obtain amine **5** (4.04 g, 84%) as a colorless liquid.

(Found: C, 82.2; H, 8.8; N, 3.9%. $C_{24}H_{31}NO$ requires C, 82.48; H, 8.94; N, 4.01). $\nu_{max.}$ (neat) 3075, 3030, 3004, 2972, 2937, 2858, 2796, 1609, 1519, 1488, 1416, 1388, 1290, 1268, 1246, 1178, 1075, 1046, 996, 918, 833, 762, and 697 cm^{-1}; δ_H ($CDCl_3$) 1.35 (2H, quint, *J* 7.4 Hz), 1.48 (4H, m), 1.80 (2H, quint, *J* 7.0 Hz), 2.43 (2H, t, *J* 7.3 Hz), 3.09 (4H, d, *J* 5.8 Hz), 3.98 (2H, t, *J* 6.6 Hz), 5.14 (4H, m), 5.86 (2H, m), 6.95 (2H, d, *J* 8.8 Hz), 7.29 (1H, t, *J* 8.0 Hz), 7.40 (2H, t, *J* 7.5 Hz), 7.51 (2H, d, *J* 8.8 Hz), 7.54 (2H, d, *J* 7.3 Hz); δ_C ($CDCl_3$) 26.02, 26.87, 27.25, 29.27, 53.23, 56.88 (2C), 67.96, 114.74 (2C), 117.30 (2C), 126.58, 126.69 (2C), 128.09 (2C), 128.68 (2C), 133.53, 135.82 (2C), 140.86, 158.67 (TMS: 0.00 ppm). DEPT 135 NMR analysis supported the ^{13}C spectral assignments.

2.2.4 Synthesis of monomer precursor 6

Dry HCl was passed through a solution of **5** (1.90 g, 5.436 mmol) in ether (30 mL) at 0-5 °C. The precipitated white salt was filtered and washed with ether to obtain **6** (2.01 g, 96%).

M.p. 108-110 °C; (Found: C, 74.4; H, 8.4; N, 3.6%. $C_{24}H_{32}ClNO$ requires C, 74.68; H, 8.36; N, 3.63). $\nu_{max.}$ (KBr) 3478, 3402, 3327, 3224, 3084, 3029, 2946, 2867, 1653, 1623, 1606, 1518, 1488, 1392, 1289, 1270, 1244, 1194, 1176, 1116, 1043, 1021, 997, 944, 848, 821, 772, 720, and 701 cm^{-1}; δ_H ($CDCl_3$) 1.42 (2H, quint, *J* 7.3 Hz), 1.53 (2H, quint, *J* 7.3 Hz), 1.80 (2H, quint, *J* 6.7 Hz), 1.89 (2H, m), 2.96 (2H, m), 3.63 (4H, m), 3.98 (2H, t, *J* 6.4 Hz), 5.52 (4H, m), 6.14 (2H, m), 6.95 (2H, d, *J* 8.6 Hz), 7.29 (1H, t, *J* 8.3 Hz), 7.41 (2H, t, *J* 7.6 Hz), 7.52 (2H, d, *J* 8.8 Hz), 7.54 (2H, d, *J* 8.3 Hz), 12.48 (1H, s); δ_C ($CDCl_3$) 23.35, 25.53, 26.53, 28.96, 51.66, 54.63 (2C), 67.53, 114.73 (2C), 125.66 (3C), 126.26, 126.63 (2C),

128.09 (2C), 128.70 (2C), 133.62, 140.72 (2C), 158.50 (TMS: 0.00 ppm). DEPT 135 NMR analysis supported the ^{13}C spectral assignments.

2.2.5 Synthesis of the resin Tetrapolymerization of monomers 6, 7, cross-linker 8 and SO_2 to hydrophobic cross-linked polyzwitterionic acid (HCPZA) 9

To a solution of **7** (5.10 g, 20 mmol), **6** (1.93 g, 5 mmol), and **8** (0.890 g, 2.78 mmol) in dimethyl sulfoxide (12.8 g) in a round bottom flask (50 cm^3) was absorbed SO_2 (1.96 g, 30.6 mmol). Initiator AIBN (250 mg) was added under N_2, then the mixture was stirred in a closed flask at 65 ºC. Within 1 h, the mixture became an immovable gel. More DMSO (6.2 g) was added, and the polymerization was continued at 67 ºC for 24 h. A few times the flask was cooled and opened to release produced N_2. Then, the obtained transparent gel was soaked in water; the white resin was repeatedly washed with water and finally with acetone. Resin HCPZA **9** was dried under vacuum at 65ºC for 6 h to a constant weight (8.55 g, 87%). The composition of the resin was found to be: C, 43.0; H, 6.8; N, 4.5; S, 10.5. The incorporated monomers in HCPZA **9** containing **7** (72.0 mol%), **6** (18.0 mol%), **8** (10.0 mol%) and SO_2 (100 mol%) requires C, 43.39; H, 6.61; N, 4.72; S, 10.82%. $\nu_{max.}$ (KBr) 3445 (br), 2920, 2854, 1635, 1518, 1483, 1467, 1410, 1310, 1249, 1128, 1029, 903, 831, 764, 699, 596, and 510 cm^{-1}.

2.2.6 Conversion of HCPZA 9 to hydrophobic cross-linked dianionic polyelectrolyte (HCDAPE) 10

Resin **9** (1.00 g, 3.0 mmol) was treated with NaOH (0.24 g, 6.0 mmol) in water (20 mL); after 1 h at room temperature, a mixture of methanol (50 mL) containing NaOH (0.12 g, 3.0 mmol) was added to the gel. The resultant HCDAPE **10** was then filtered, washed with methanol and dried under vacuum for 6 h at 65 °C (1.05 g, 99%).

The composition of the resin was found to be: C, 40.7; H, 5.9; N, 4.2; S, 9.6. The incorporated monomers as in HCDAPE **10** containing repeating units derived from **7** (72.0 mol%), **6** (18.0 mol%), **8** (10.0 mol%) and SO_2 (100 mol%) requires C, 41.07; H, 5.73; N, 4.35; S, 9.96%. $\nu_{max.}$ (KBr) 3430, 2924, 2784, 1667, 1611, 1521, 1487, 1416, 1308, 1245, 1182, 1125, 1049, 972, 834, 765, 695, 552, and 499 cm^{-1}.

2.2.7 Swelling coefficient

The swelling coefficient was evaluated as follows: resins were crushed and a 20- to 30-mesh fraction was used. The coefficient of swelling is defined as the ratio of the settled wet volume of the resin to the dry volume. Thus, to a known volume of dry resin in a burette, sufficient water was added to cover the resin and the volume of the wet resin was measured and compared with the volume of the dry resin. After no further change in the volume occurred, the volume of the wet resin was recorded.

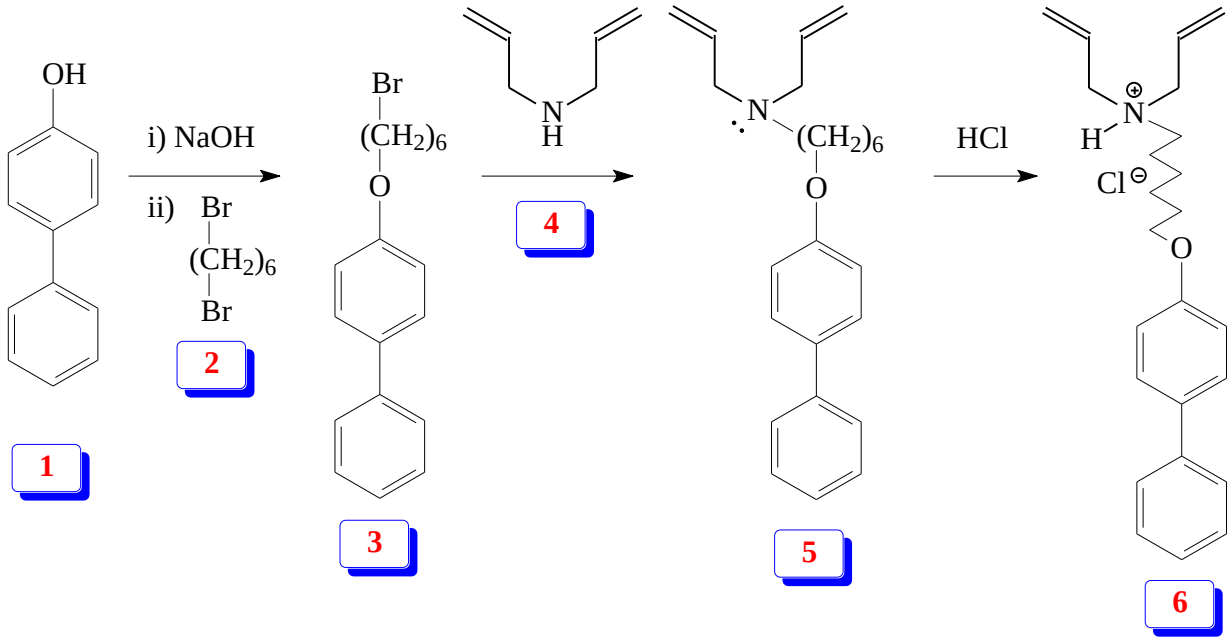

Figure 2.1 Synthesis of hydrophobic monomer 6

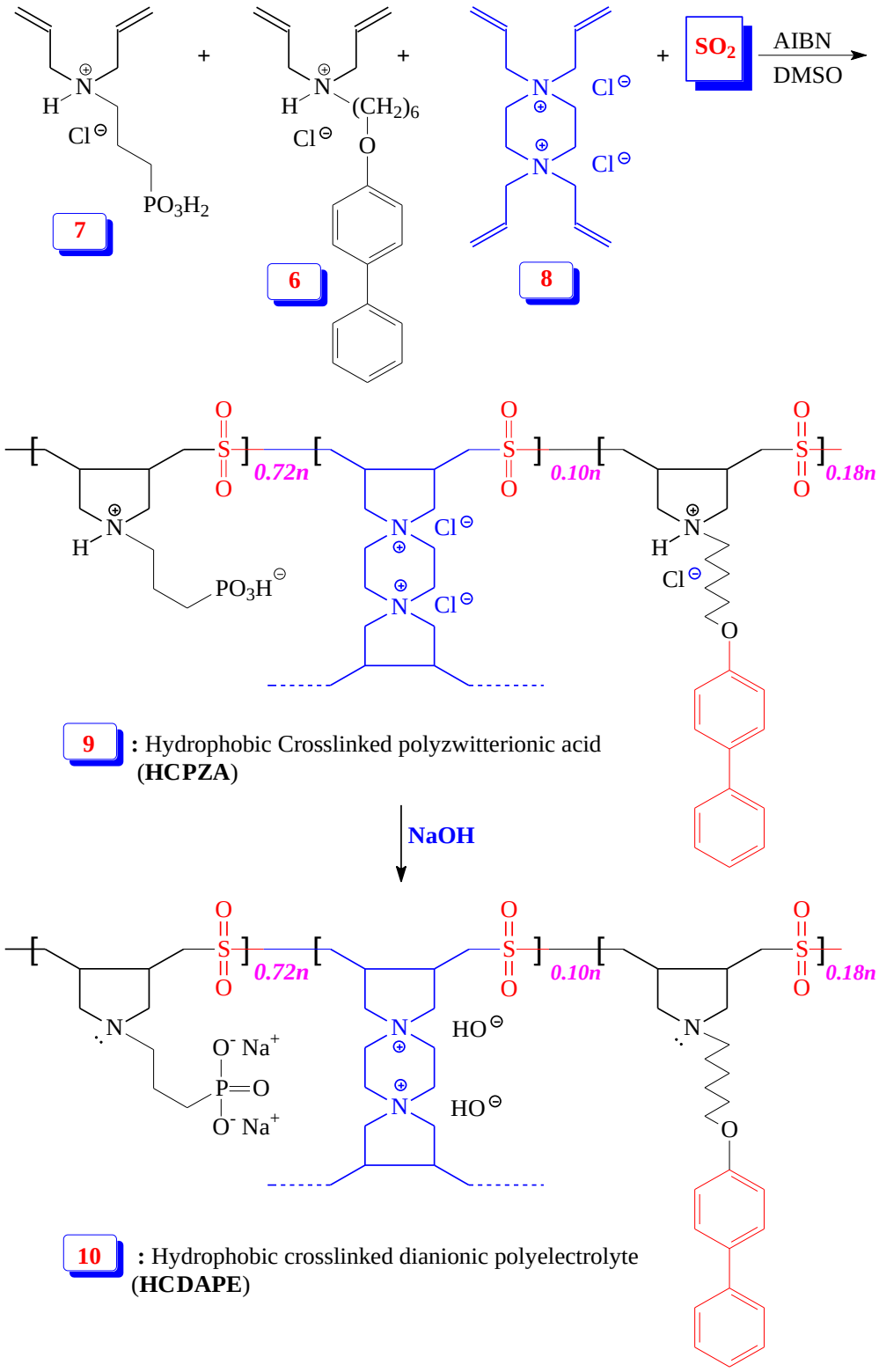

Figure 2.2 Synthesis of a hydrophobic cross-linked polyzwitterion/anion resins

2.2.8 Adsorption experiment

Adsorption experiments were performed using solutions with a known concentration of methylene blue, mercury(II) or a mixture of both in a container containing a predetermined amount of the resin and placed on a shaker at a predetermined rpm speed. The pH of the solution was adjusted with HNO_3 and NaOH solutions using a pH meter. The dye concentration was determined by UV–Vis spectrophotometer while the concentration of the Hg(II) was monitored using mercury analyser. The experiments were executed at room temperature (25 °C). The influence of the parameters (i.e. pH, dosage, initial concentration, shaking speed and temperature) controlling the adsorption were optimized using central composite design (CCD) which is the most popular response surface method (RSM) design. This approach helps us to investigate the effect of parameters in a cost- and time-effective way consuming less amount of material so as to be environmentally friendly.

2.2.9 Kinetic and Isotherm studies

The kinetic studies were performed under the optimum conditions of shaking speed (150 rpm) and pH (5). Containers containing a mixture of the adsorbates and resin were agitated in a shaker at 25 ^{o}C and aliquots were collected at time intervals of 2, 5, 10, 20, 30, 40, 50, 60, 70, 80, 90 and 120 min. After the equilibrium, final methylene blue concentration was analyzed using UV–Vis spectrophotometer and the Hg concentration was analyzed by a mercury analyzer. The adsorption capacity for (q_e) was calculated using the equations:

$$q_e = (C_o - C_e) \times \frac{V}{m} \qquad (1)$$

where *V* stands for the volume of the solutions (mL) and *m* is the mass in gram (g) of adsorbent. All the experiments were performed in duplicate and the relative standard deviation was lower than 3.0%. The values of kinetic and isotherm parameters were determined by a linear regression analysis.

2.3 Results and discussion

2.3.1 Characterization of the polymer

New hydrophobic monomer **6** was synthesized as outlined in **Figure 2.1** in excellent yield. Thus, *p*-Phenylphenol (**1**) was alkylated with 1,6-dibromohexane (**2**) to **3** which on treatment with diallyl amine afforded monomer precursor **5** in 84% yield. Monomer **6** was then obtained by treating **5** with gaseous HCl in 96% yield. The monomer was characterized by elemental and spectral analyses: ^{1}H and ^{13}C NMR spectra (**Figure 2.3**) confirmed its structure. The chemical shifts were assigned based on substituent effects; the spectrum revealed each and every carbon signals (**Figure 2.3b**).

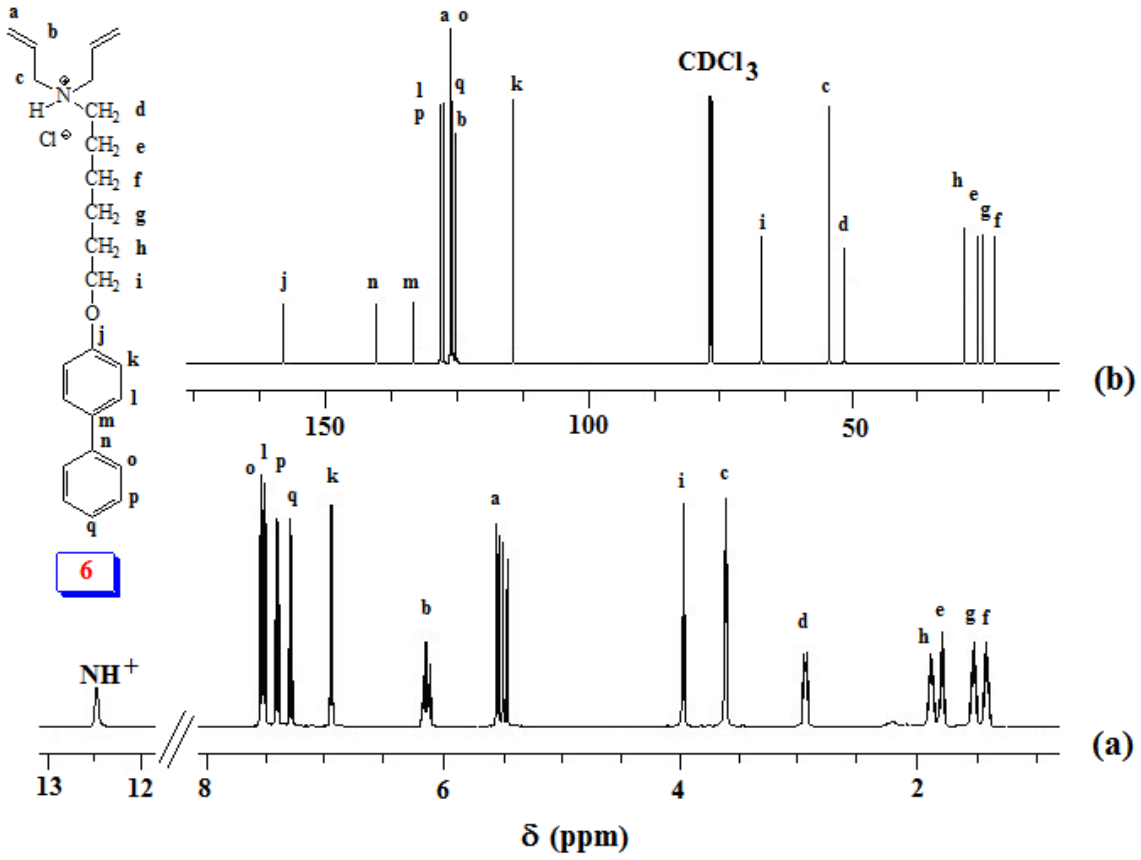

Figure 2.3 1H and 13C NMR spectra of monomer 6

Butler's cyclopolymerization protocol [19-22] was exploited in the AIBN-initiated tetrapolymerization of hydrophobic monomer **6**, hydrophilic monomers **7** and cross-linker **8**, along with alternating SO_2 as the fourth monomer to obtain hydrophobic cross-linked polyzwitterionic acid (HCPZA) **9** in 87% yield. During work up, HCl is eliminated to give the zwitterionic aminophosphonate motifs. The composition of the repeating units in the resin matched with the feed ratio of 0.18 : 0.72 : 0.10 : 1.0 for monomers **6**/**7**/**8**/SO_2 as supported by elemental analysis: This is expected for such a high conversion to the polymer (in 87% yield). The incorporation of hydrophobic monomer was confirmed by solid-state

^{13}C NMR spectrum which revealed the presence of carbon signals in the aromatic region (110-150 ppm) (**Figure 2.4**).

HCPZA **9** upon treatment with NaOH was converted to HCDAPE **10.** Zwitterionic resin **9** and its anionic form **10** were found to have swelling coefficients of 2.2 and 5.8, respectively. The zwitterionic form in a compact coil is expected to have a lower affinity for adsorption of water, while anionic form **10** has more expanded conformations owing to repulsion among negative charges and thus has a greater affinity for solvation.

Note that the incorporation of the hydrophobic monomer into the cross-linked polymer would serve dual purposes: simultaneous removal of toxic metals as well as organic contaminants from wastewater. In a single treatment, it would exploit the chelating ability of aminophosphonate ligand to capture metal ions and the hydrophobic surface of long chain hydrocarbons to scoop up the organic contaminants. We did anticipate an exciting outcome.

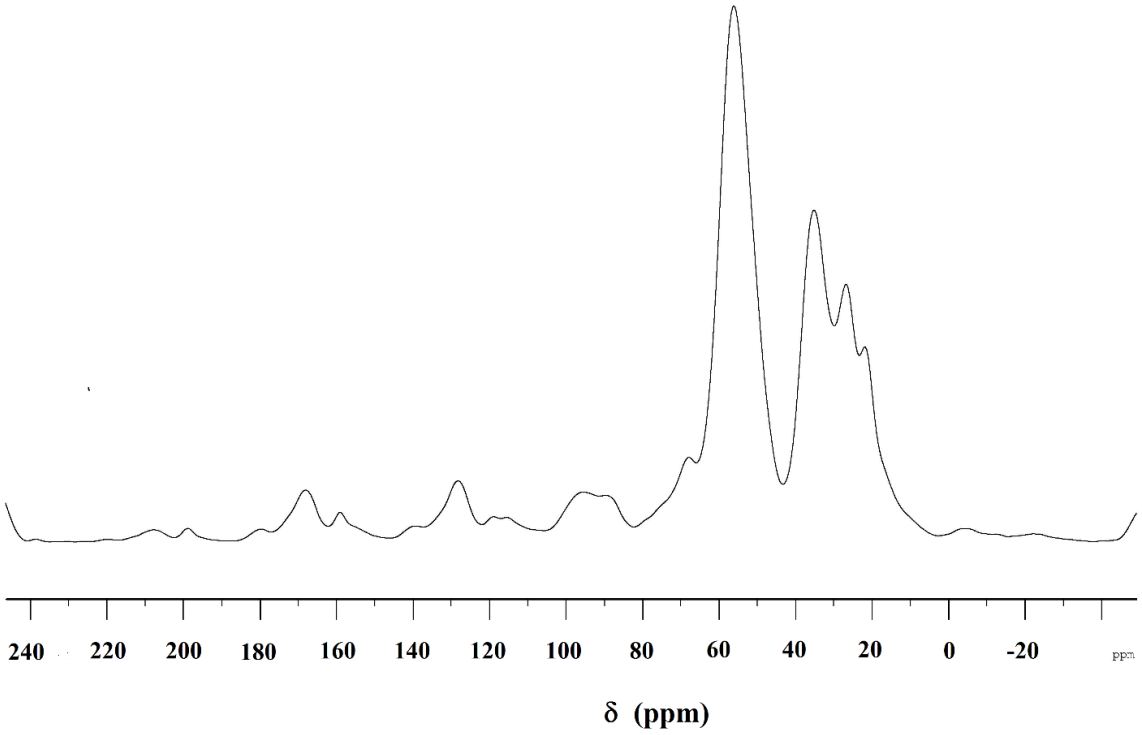

Figure 2.4 ^{13}C solid NMR of HCPZA 9

The IR spectrum was obtained for the polymer in acid and basic forms as depicted in **Figure 2.5**. The spectra show bands at ≈1310 cm^{-1} and ≈1125 cm^{-1} which can be assigned to asymmetric and symmetric bands of SO_2 [23]. Phosphonate groups from intensive IR absorption bands at 560 – 600 cm^{-1} and 1000 – 1100 cm^{-1} regions. Adsorbed water band can be seen at around 3400 cm^{-1} of the polymer in acidic form **9** and at the relatively wide range, from 2600 to 3600 cm^{-1}; the polymer in basic form **10** displayed an explicit peak at 3470 cm^{-1} and a weaker peak is also found at 630 cm^{-1}. The bands at around 1600-1680 cm^{-1} can be assigned to the C=C stretching.

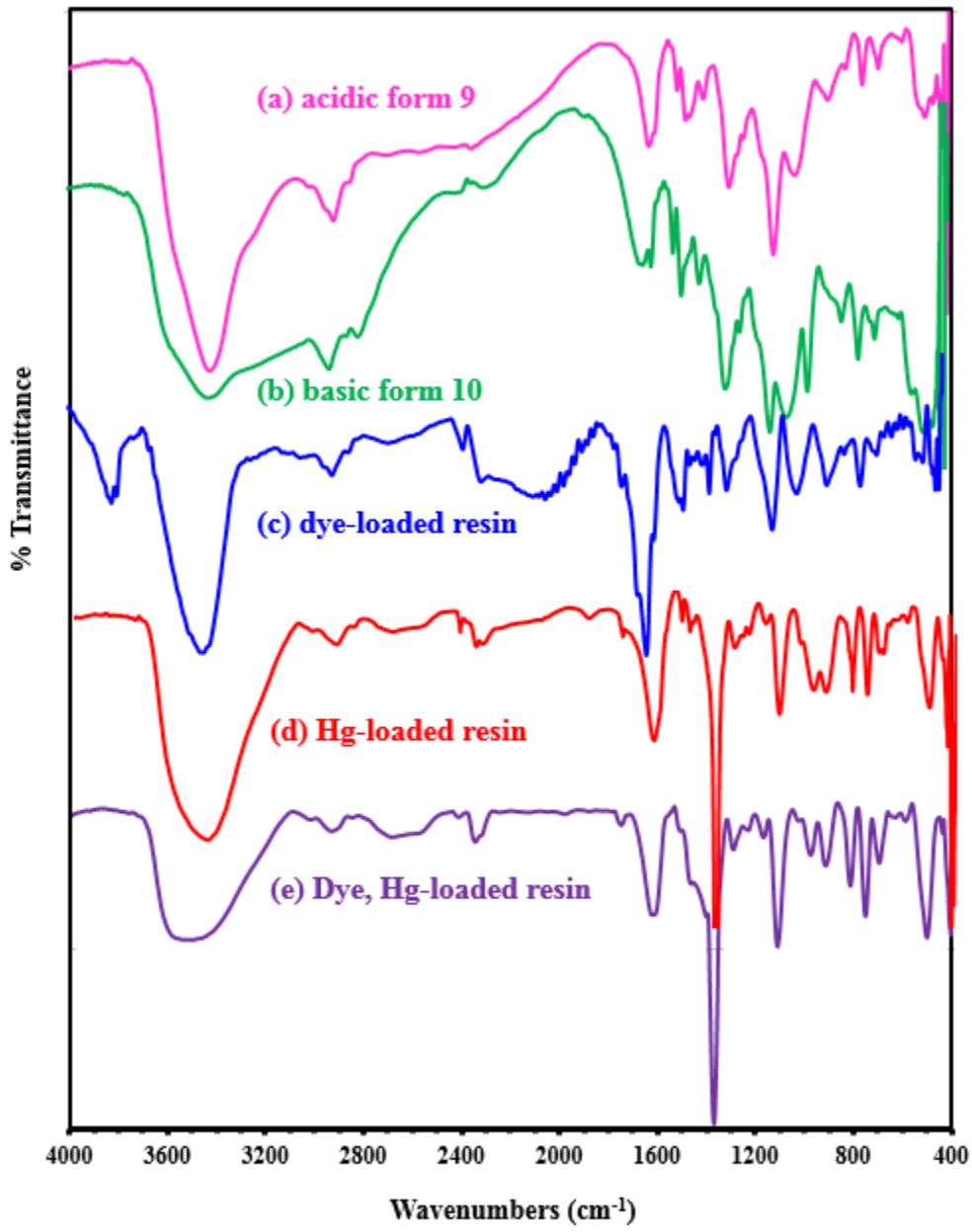

Figure 2.5 IR Spectra of the cross-linked polymer (a) in acidic form 9 (b) in basic form 10.; IR Spectra of (c) dye-loaded resin 9, (d) Hg-loaded resin 9 and (e) Dye, Hg-loaded resin 9

The TGA curve of **9**, shown in **Figure 2.6**, revealed two distinct weight loss steps. The first slow but gradual weight loss of about 13% is attributed to the removal of moisture and

water molecules embedded in the cross-linked polymer. The second dramatic loss of about 70% around 335 °C is attributed to the loss of phosphonate pendants and SO_2 owing to polymer degradation. It could also attribute to the combustion of nitrogenous organics with the release of NOx, CO_2, and H_2O gasses [23]. The polymer remained stable even at 250 °C. The DSC curve indicates that there is a crystalline melt defined by the peak temperature at around 350 °C.

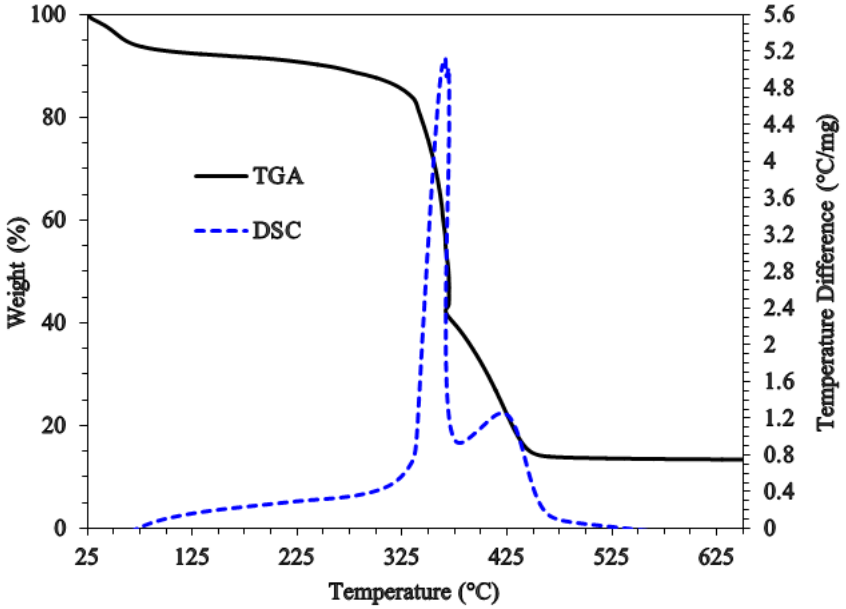

Figure 2.6 TGA curves of HCPZA 9

2.3.2 Characterization Results of the factorial design

Central composite design (CCD), which is the most popular response surface method (RSM), was implemented to design a series of tests with least number of experiments. This approach helped us to investigate the effect of parameters involved (i.e. pH, dosage, initial concentration, shaking speed and temperature) on the responses (i.e. the removal percentage) in a cost- and time-effective way. It also helped to consume less amount of

material to make the process environmentally friendly. The CCD makes it feasible to observe the possible interaction of the parameters and their influences on the removal efficiency. The experimental factors that have been included are pH (3-7), adsorbent dosage (10 – 30 mg), initial concentrations (0.1-10 µM dye and 10-70 ppm Hg(II)), shaking speed (50-150 rpm) and temperature (25-65 ^{o}C) with 95% confidence limit. The design of experiment (DOE) is considered more informative than one-variable-at-a-time experimental procedures since it gives an indication of the interaction between the factors. The low and high levels of initial Hg(II) concentrations were selected to stimulate the real industrial wastewaters. The type of design was 2-level factorial (default generators) (**Table 2.1).** Based on the experimental design, the adsorption tests were performed using adsorbent **9**. The percentage removal of the Hg or dye under certain conditions is the response variable in this study.

The factorial design plots, including Pareto chart and normal plot of the effects, are depicted in **Figure 2.7.** The Pareto chart indicates that the most significant factors influencing the adsorption of dye on the prepared adsorbent are initial concentration, shaking speed and dosage. The half-normal plot of the effects indicates that the removal of dye increases with increasing the pH of the solution while at low dye concentration the percentage removal was high. There was a decrease in the removal by increasing the temperature though the change was relatively insignificant. The interaction plot for the response, **Figure 2.7c** indicates that the interaction between the dosage, initial concentration and shaking speed have the highest effect on the adsorption of dye. The interaction between the media pH and the initial concentration was also significant in affecting the removal efficiency.

Considering the optimization of parameters for the Hg(II) adsorption, the Pareto chart, **Figure 2.8a** indicates that the most significant factors influencing the adsorption of Hg(II) on the resin are initial concentration, temperature and shaking speed. The half-normal plot of the effects indicates that the highest removal was obtained at high pH (studied in the range 3-7, **Table 2.1**) with increasing the shaking speed. By increasing the temperature, the removal was enhanced. The interaction plot for the response, **Figure 2.8c** indicates that the highest interactions between the experimental factors were the interaction between the temperature and dosage followed by the interaction between initial concentration and temperature.

Table 2.1 Design matrix of the factorial design in the central composite design (CCD)

Variable	Low(-)	Central point (0)	High(+)
Parameters optimization for dye removal			
pH	3	5	7
Adsorbent dosage (mg)	10	20	30
Initail concentration (μM)	0.1	5.05	10
Shaking speed (rpm)	50	100	150
Temperature (^{o}C)	25	45	65
Parameters optimization for Hg removal			
pH	3	5	7
Adsorbent dosage (mg)	10	20	30
Initail concentration (ppm)	10	40	70
Shaking speed (rpm)	50	100	150
Temperature (K)	25	45	65

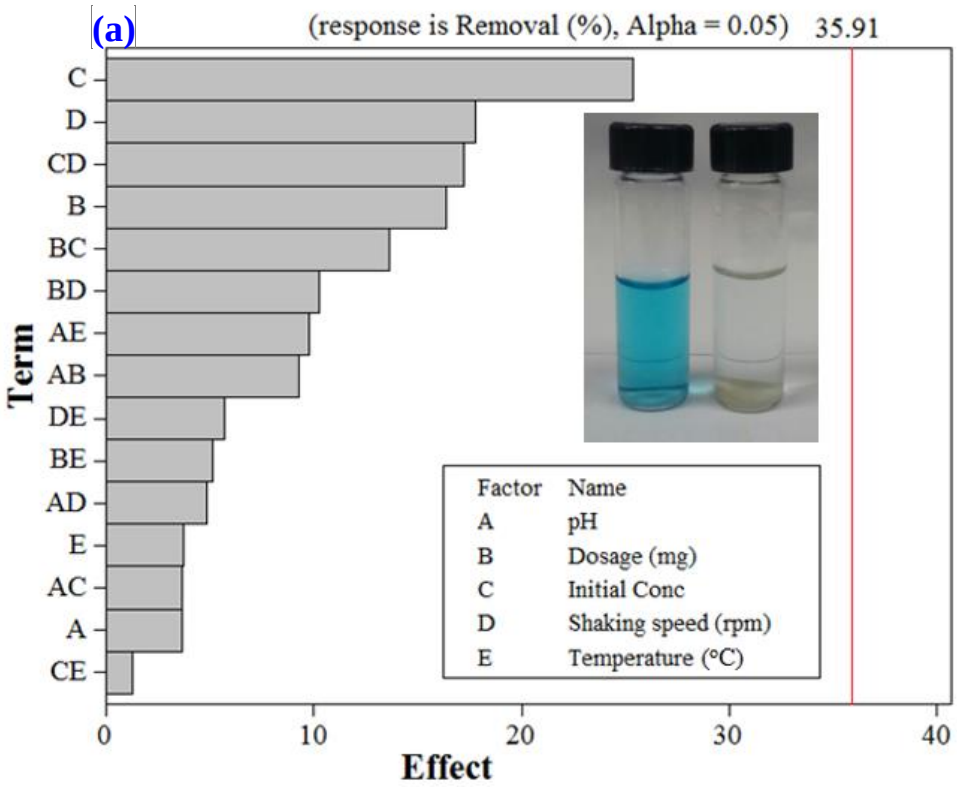
(a)
(response is Removal (%), Alpha = 0.05)
35.91
C
D
CD
B
BC
BD
AE
AB
DE
BE
AD
E
AC
A
CE
Term
0
10
20
30
40
Effect
Factor Name
A pH
B Dosage (mg)
C Initial Conc
D Shaking speed (rpm)
E Temperature (°C)

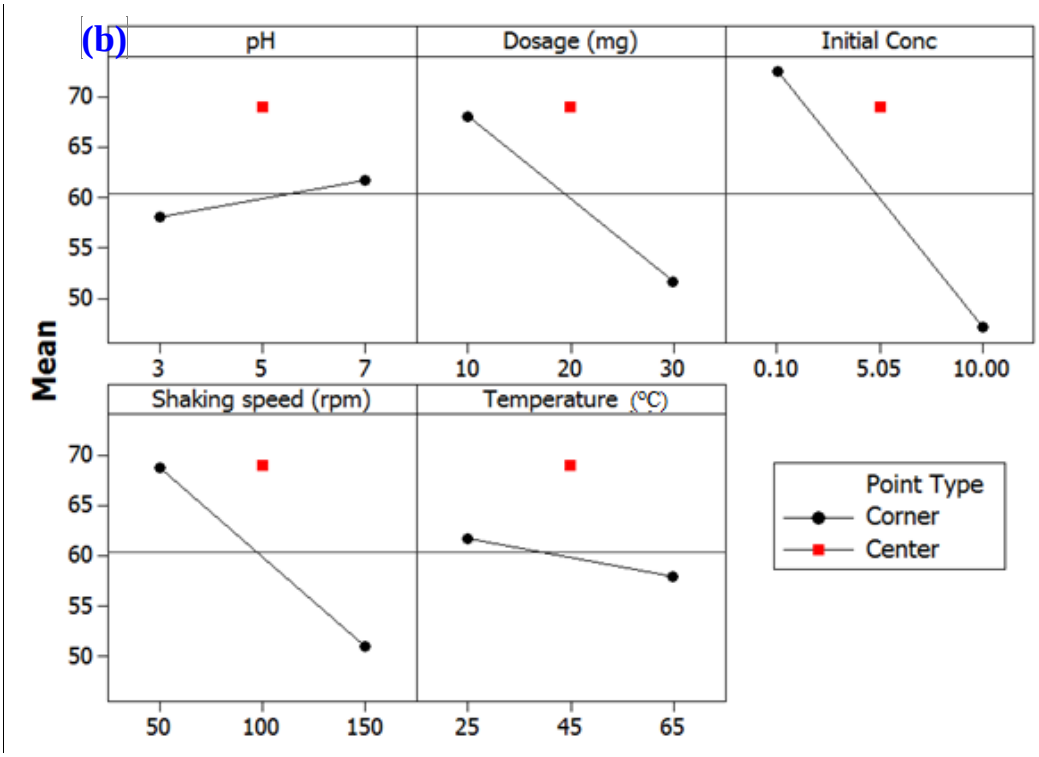
(b)
pH
Dosage (mg)
Initial Conc
Shaking speed (rpm)
Temperature (°C)
Mean
70
65
60
55
50
3
5
7
10
20
30
0.10
5.05
10.00
50
100
150
25
45
65
Point Type
Corner
Center

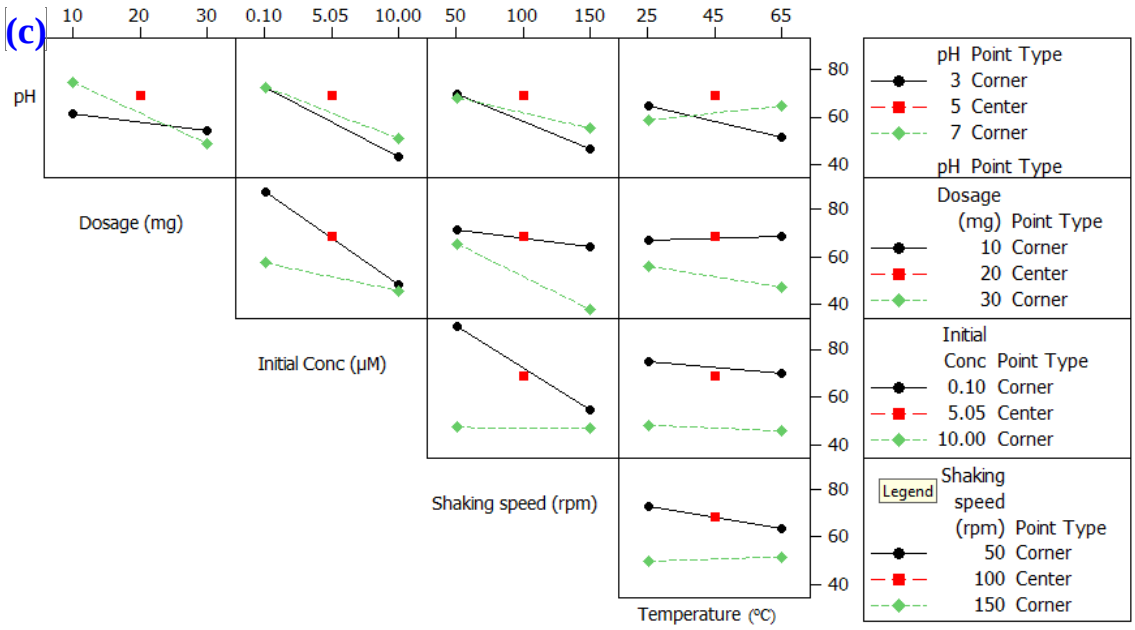

Figure 2.1 The factorial design for the optimization of adsorption of dye showing; (a) Pareto chart, (b) the half-normal plot of the effects; (c) The factorial design showing the interaction plot for a response

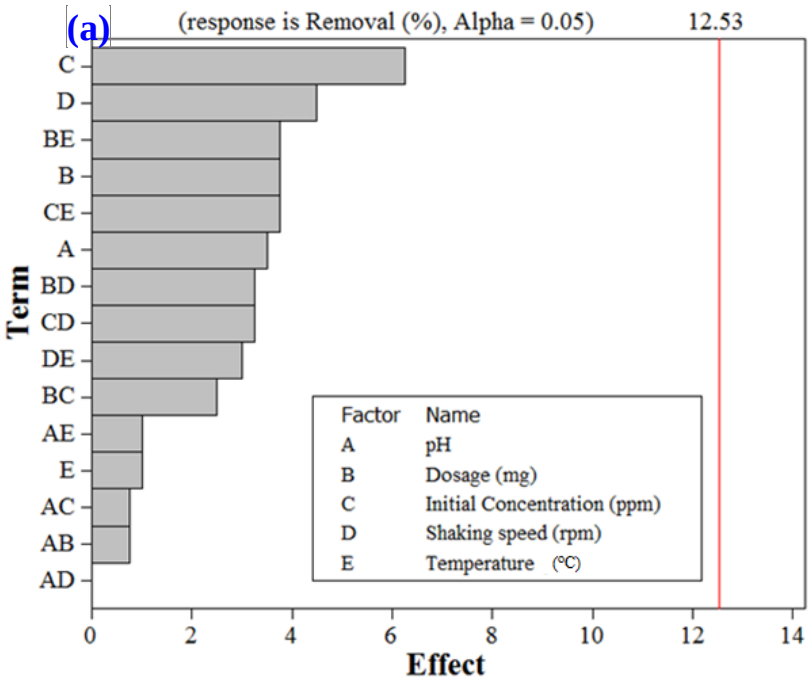

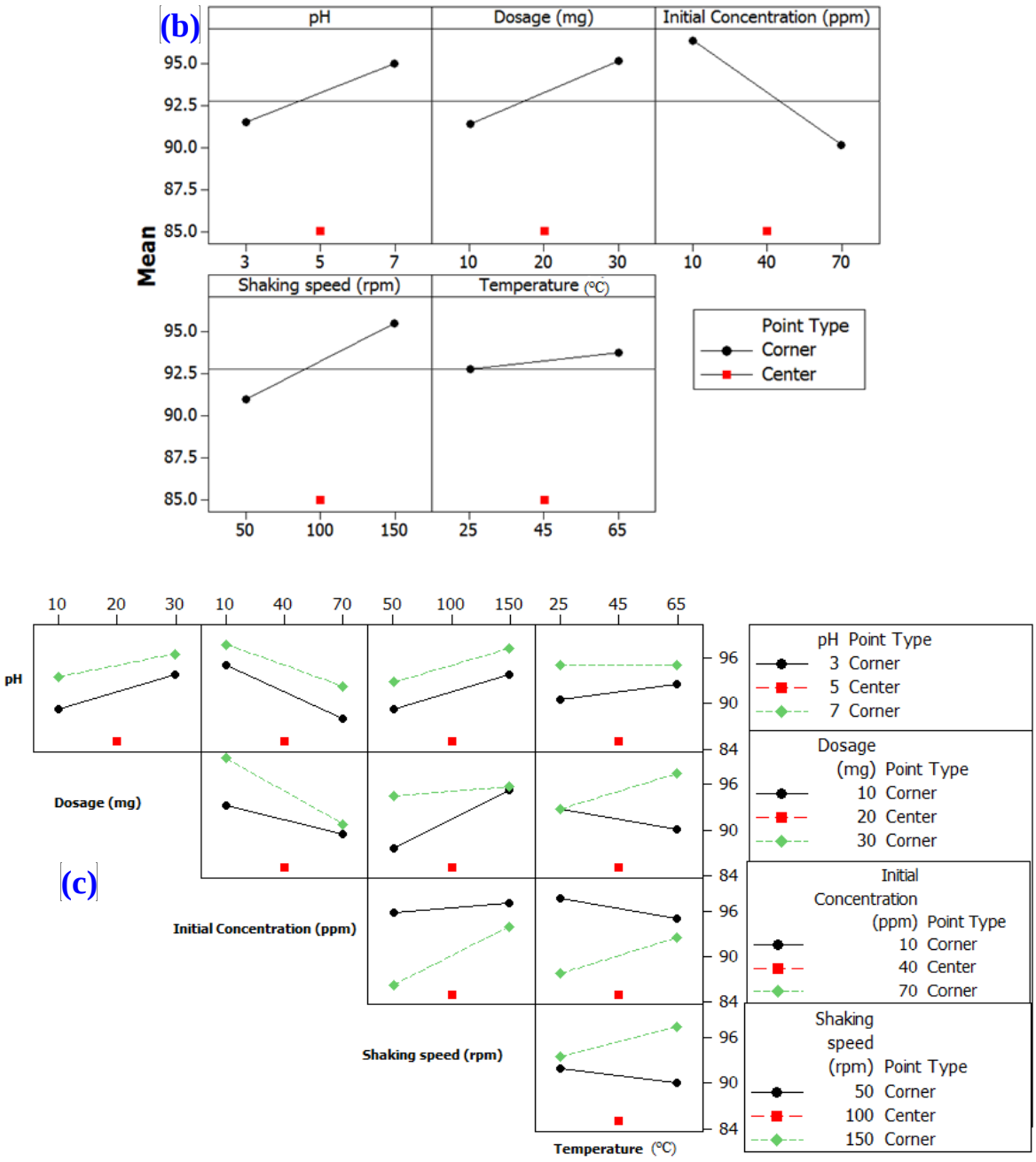

Figure 2.2 The factorial design for the optimization of adsorption of Hg(II) showing; (a) Pareto chart, (b) the half-normal plot of the effects; (c) The factorial design showing the interaction plot for a response

2.3.3 Adsorption kinetics

Lagergren's first-order and pseudo-second-order kinetics model were implemented to examine the controlling mechanism of mercury and methylene blue adsorption from aqueous solutions. Adsorption equilibrium was reached in 40 min. The linear equation for Lagergren's first order kinetics is given as [24]:

$$\ln(q_e - q_t) = \ln q_e - k_1 t \qquad (2)$$

First order kinetics using q_t with contact time for the removal of the dye and Hg by the resin for different feed concentrations; indicates that the experimental data do not fit with the first order model (**Table 2.2**). Therefore, the experimental data were evaluated using the pseudo-second adsorption kinetic rate equation [25]:

$$\frac{dq_t}{dt} = k_2(q_e - q_t)^2 \qquad (3)$$

k_2 depicted the rate constant of the pseudo-second order adsorption (g/mg.min), q_e and q_t are the adsorbed amount (capacity) of Hg(II) at equilibrium and at time t.

The linear form of pseudo-second-order is written as:

$$\frac{t}{q_t} = \frac{1}{k_2 q_e^2} + \frac{t}{q_e} \qquad (4)$$

where q_e and q_t are the adsorption capacities at equilibrium and at time t (min) respectively. k_2 (g/(mg.min)) is the pseudo-second-order rate constant. The values of q_e and k_2 can be calculated from the slope and intercept of the plot of t/q_t versus t. The results listed in **Table 2.2** show high correlation coefficient ($R^2 \geq 0.99$), which suggest that the kinetics data were better described with a pseudo-second-order kinetics model. The adsorption capacity was determined as a function of adsorbate initial concentration and adsorbent dosages. The

calculated equilibrium adsorption capacities were in consistent with the obtained experimental results. Screening the literature, it was found that the equilibrium adsorption capacities of methylene blue and Hg on the reported polymeric adsorbent were relatively close to that on various adsorbents reported in the literature, considering low initial concentrations ranges [8, 9, 12, 15].

Table 2.2 Adsorption kinetic parameters for Lagergren models

Adsorbate		Lagergren's first order			Pseudo-second order			
	$q_{e,exp}$ (mg g^{-1})	k_1 (min^{-1})	$q_{e,cal}$ (mg g^{-1})	R^2	$q_{e,cal}$ (mg g^{-1})	k_2 (g $mg^{-1}min^{-1}$)	H[a]	R^2
3.2 ppm MB[b]	2.54	0.04	8.25	0.8542	2.86	0.61	1.44	0.9980
3.2 ppm MB mixed with 10 ppm Hg (II)	2.85	0.03	6.01	0.8774	2.95	0.25	1.56	0.9971
0.32 ppm MB [c]	1.95	0.06	4.08	0.7692	2.10	0.23	1.92	0.9968
0.32 ppm of MB mixed with 10 ppm	2.03	0.07	3.98	0.9807	2.05	0.35	1.23	0.9965
10 ppm Hg	7.01	0.05	5.25	0.8835	7.31	0.36	1.63	0.9989
10 ppm Hg mixed with 3.2 ppm MB	7.85	0.06	6.85	0.9781	8.10	0.72	1.01	0.9988
70 ppm Hg	55.3	0.09	8.84	0.9879	56.01	0.62	1.27	0.9991
70 ppm Hg mixed with 3.2 ppm MB	58.2	0.08	7.52	0.8968	57.85	0.65	1.48	0.9958

[a] Initial adsorption rate, $h = k_2 q_e^2$
[b] i.e. 1×10^{-5} M of MB,
[c] i.e. 1×10^{-6} M of MB

2.3.4 Adsorption isotherms

It is imperative to describe the mechanism associated with the adsorption process by which the adsorbate is adsorbed. The equilibrium data of dye, Hg and the mixture of both were evaluated by Langmuir and Freundlich isotherms. The Langmuir isotherm postulates a monolayer adsorption which takes place at binding sites with, no interactions between the molecules adsorbed and neither is the transmigration on the surface of the sorbent [26]. The Langmuir equation is given by Eq. (5)

$$\frac{C_e}{q_e} = \frac{1}{k_L q_m} + \frac{C_e}{q_m} \qquad (5)$$

where q_m (mg/g) is the quantity of monolayer adsorbate required to form a single monolayer on a unit mass of the adsorbent ($mg \bullet g^{-1}$), q_e is the amount adsorbed on a unit mass of adsorbent ($mg \bullet g^{-1}$) at equilibrium concentration C_e ($mg \bullet L^{-1}$) and k_L is Langmuir equilibrium constant ($L \bullet mg^{-1}$) that takes care of the apparent energy of adsorption. A plot of C_e/q_e against C_e yielded a straight line in agreement with Langmuir isotherm giving the isotherm parameters as presented in **Table 2.3**.

The values of Langmuir constants q_m and k_L were calculated from the slope and intercept of the plot, and are given in **Table 2.3**. From the data, the R^2 values, it is apparent that the adsorption fitted relatively well with the Langmuir Isotherm model. The characteristic parameter of the Langmuir isotherm is demonstrated in terms of dimensionless equilibrium parameter R_L, also defined as separation factor, by Weber and Chakkravorti [27]:

$$R_L = \frac{1}{1 + K_L C_o} \qquad (6)$$

where C_o is the initial solute concentration. The value R_L gives an indication of the type of the isotherm and the nature of the adsorption process. It indicates whether the adsorption nature is either unfavorable (R_L>1), linear (R_L =1), favorable (0< R_L<1) or irreversible (R_L = 0). From the data calculated and presented in **Table 2.3**, the R_L values between zero and 1 indicate the favorable nature of the adsorption [28]. Considering the interactions between the adsorbed molecules, the Freundlich model is utilized to describe the adsorption characteristic on heterogeneous adsorbent surface, using the empirical equation:

$$q_e = K_f C_e^{\frac{1}{n}} \qquad (7)$$

where k_F (mg•g^{-1}) is the Freundlich isotherm constant indicating adsorption capacity and n is the adsorption intensity while 1/n is a function of the strength of the adsorption, C_e is the equilibrium concentration of adsorbate (mg•L^{-1}) and q_e is the amount of adsorbate per adsorbent at equilibrium (mg•g^{-1}). The logarithmic form of Freundlich is defined as:

$$\ln q_e = \ln K_f + \frac{1}{n} \ln C_e \qquad (8)$$

From the plot of Ln q_e versus Ln C_e, K_F and n were calculated **Table 2.3**. The *n* values give an indication of the favorability of the adsorption process. The value of $n > 1$ represents a favorable adsorption. A value of $1/n < 1$ indicates a normal adsorption while $1/n > 1$ indicates a cooperative adsorption. In this study, the value of $1/n$ is less than 1 indicating a favorable adsorption process of the dye and Hg on the polymer. The k_F and R^2 values in **Table 2.3** show that the Freundlich model gives the best fit for the four systems studied.

The data were fitted to the Dubinin-Radushkevich (D-R) isotherm model applied to the data to deduce the heterogeneity of the surface energies of adsorption and the characteristic porosity of the polymer. The linear form is:

$$\ln q_e = \ln q_D - B_D[RT\ln(1+1/C_e)]^2 \qquad (9)$$

The apparent energy of adsorption was calculated as:

$$E=1/(2B_D)^{1/2} \qquad (10)$$

where q_D is the D-R constant indicating the theoretical saturation capacity and B_D is a constant or the mean free energy of adsorption, R is the ideal gas constant, (8.314J/molK), T (K) is the temperature of adsorption and E is the mean free energy of adsorption per molecule of the adsorbate when transferred to the surface of the solid from infinity in solution. From the plot of $\ln q_e$ against $[RT\ln(1+1/C_e)]^2$, the constants q_D and B_D were calculated from the intercept and slope and E was calculated from the obtained B_D.

If the value of E lies between 8 and 16 kJ/mol the sorption process is a chemisorptions process, while values below 8 kJ/mol indicate a physical adsorption process [29, 30]. The value of the apparent energy of adsorption in **Table 2.3** indicated a tendency towards chemisorption for the Hg(II) adsorption (E≈ 8 kJ/mol) and physisorption for the MB.

Table 2.3 Langmuir and Freundlich isotherms data for adsorption by HCPZA 9

Adsorbate	Langmuir isotherm				Freundlich isotherm				Dubinin – Radushkevich isotherm			
	q_m (mg•g^{-1})	k_L (L•mg^{-1})	R_L	R^2	1/n	n	K_f (mg•g^{-1})	R^2	q_d (mg/g)	B_D (mol^2/kJ)	E *(KJ/mol)*	R^2
MB	14.9	0.03	0.02	0.9703	1.12	0.89	13.5	0.9799	42	0.013	6.2	0.9867
Hg	31.5	0.35	0.04	0.9907	1.01	0.99	29.5	0.9980	53	0.009	7.5	0.9878
MB mix	22.71	0.08	0.06	0.9981	2.08	0.48	23.5	0.9987	46	0.023	4.6	0.9988
Hg mix	35.0	0.45	0.04	0.9658	1.96	0.51	38.0	0.9899	56	0.008	7.9	0.9869

2.3.5 Characterization of the polymer after sorption

The analysis of the adsorbate loaded polymer was conducted using SEM, EDX, IR and XPS. The polymer was collected after adoption by separation. The photos depicted in **Figure 2.9** show the change in the resin color because of the interaction between the dye or Hg with the adsorbent. Comparing the SEM/EDX results of the resin before and after the adsorption of dye and Hg, one can notice the presence of the mercury in the EDX spectrum at 21 and 88 keV. The amount of the nitrogen was also increased indicating the presence of the dye on the surface as methylene blue contains nitrogen in the structure. The mercury and nitrogen mapping give some indication of the adsorbate distribution on the resin. The data confirm the possible binding of Hg(II) to the surface of the polymer.

As depicted in **Figure 2.10**, the mercury immobilization on the surface is examined by XPS spectra of the resin before and after the adsorption of Hg(II). A new peak at 101 eV corresponding to Hg (4f) orbital appears after the mercury contact [31, 32].

In the dye loaded resin, the amplified C=C stretching vibration at 1600 cm^{-1} confirms the adsorption of the dye since both the resin and dye show vibration at 1600 cm^{-1} (*cf*. **Figure 2.5: a *vs*. c**). Comparisons between the spectra of the Hg(II)-loaded resin and pristine resin indicate a hypsochromic shift and decrease of some wavenumbers for the bands of the resin indicating the chelation between the phosphonate groups and the mercury ions [33] (*cf*. **Figure 2.5a vs. 2.3d**).

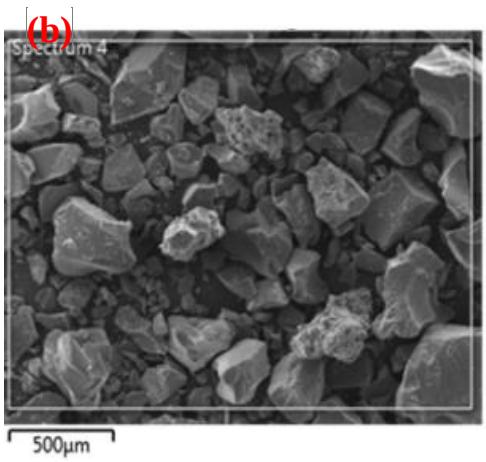

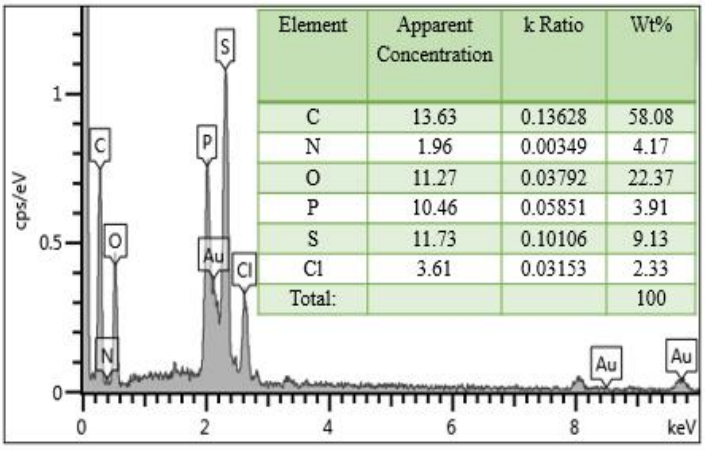

Element	Apparent Concentration	k Ratio	Wt%
C	13.63	0.13628	58.08
N	1.96	0.00349	4.17
O	11.27	0.03792	22.37
P	10.46	0.05851	3.91
S	11.73	0.10106	9.13
Cl	3.61	0.03153	2.33
Total:			100

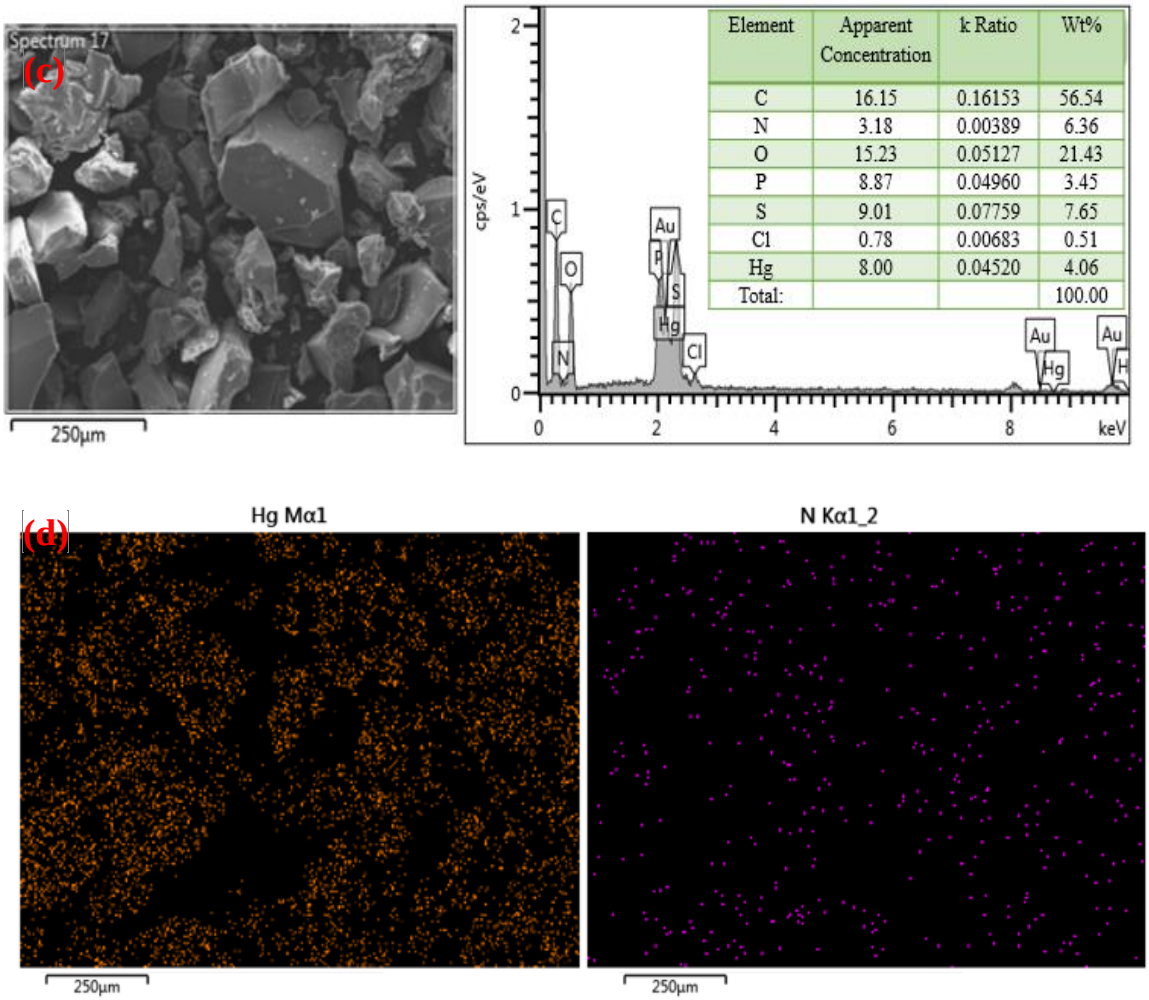

Figure 2.3 (a) photo of the resin, dye-loaded resin, Hg-loaded polymer, and dye and Hg-loaded polymer; (b) SEM image and EDX spectrum of the prepared polymer; (c) SEM image and EDX spectrum of the dye&Hg-loaded resin

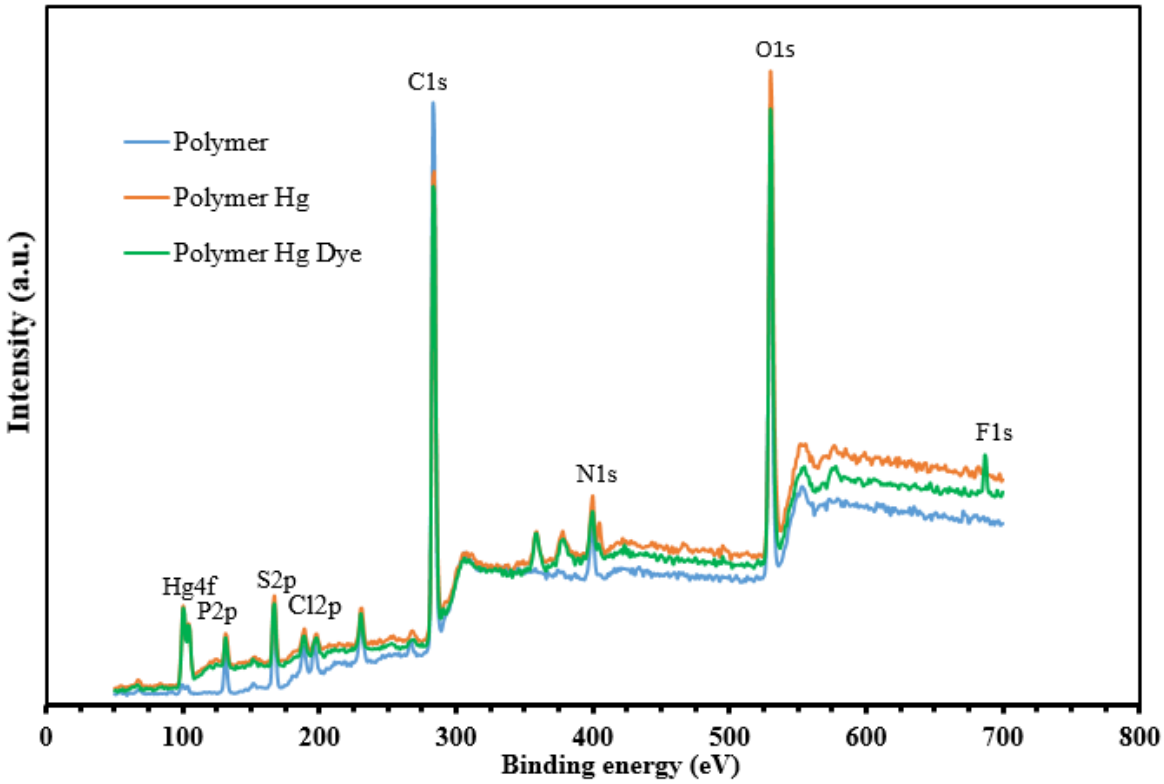

Figure 2.4 X-ray photoelectron spectroscopy (XPS) spectra of the pristine polymer sample, Hg(II)-loaded polymer and Hg-dye-loaded polymer after adsorption

2.3.6 Immobilization mechanism

The three pK_a values for the triportic species **A** are expected to be around 10.5, 6.0 and 2.4 [34, 35]. The adsorption capacities of Hg(II) is increased with the increase of the solution pH values, particularly in the pH range of 1.0−5.0. The larger concentrations of H^+ ions at lower pH values push the A ⇌ B equilibrium towards left. With increasing pH values, the formation of **B** is preferred. In the entire pH window, the cross-linker units will have cationic charges which can bind NO_3^-. The presence of new bands around 1383 cm^{-1} (**Figure 2.5d**) due to nitrate group suggests the ability of the resin to act also as an anion-exchanger [36, 37]. At higher pH values, increased negative charge density on the polymer

pendants would encourage ion exchange as well as complexation via bidentate ligand to give species to give **D**. The chelating functionality of aminopropylphosphonate may also act as a tridentante ligand as depicted in **E** [38]. It is worth mentioning that sulfone motifs are also known to act as ligands in metal ion complexes [39, 40]. The study at pH >5 is avoided since the uptake of Hg(II) cannot be attributed only to the interaction of the Hg(II) ions with the active sites on the resin. The formation of insoluble $Hg(OH)_2$ would lead to erroneous data on the adsorption [41].

MB is a weakly basic cationic dye with a pK_b of 10.2. While the dye is soluble in water, it can also display hydrophobic interaction because of having two $-N(CH_3)_2$ groups. The attractive interactions between the MB molecules may lead to possible multilayer adsorption. Owing to resonance, the highly dispersed positive charge in MB is expected to have weak ionic/electrostatic interaction with anionic $-PO_3H^-$ motifs in the resin. Hg(II) can form a bond with MB as depicted in **F** which co-adsorbs on the resin surface [42]. The adsorption of MB may well be augmented *via* hydrophobic interaction and π–π stacking as depicted in **G** (**Figure 2.11**) [43].

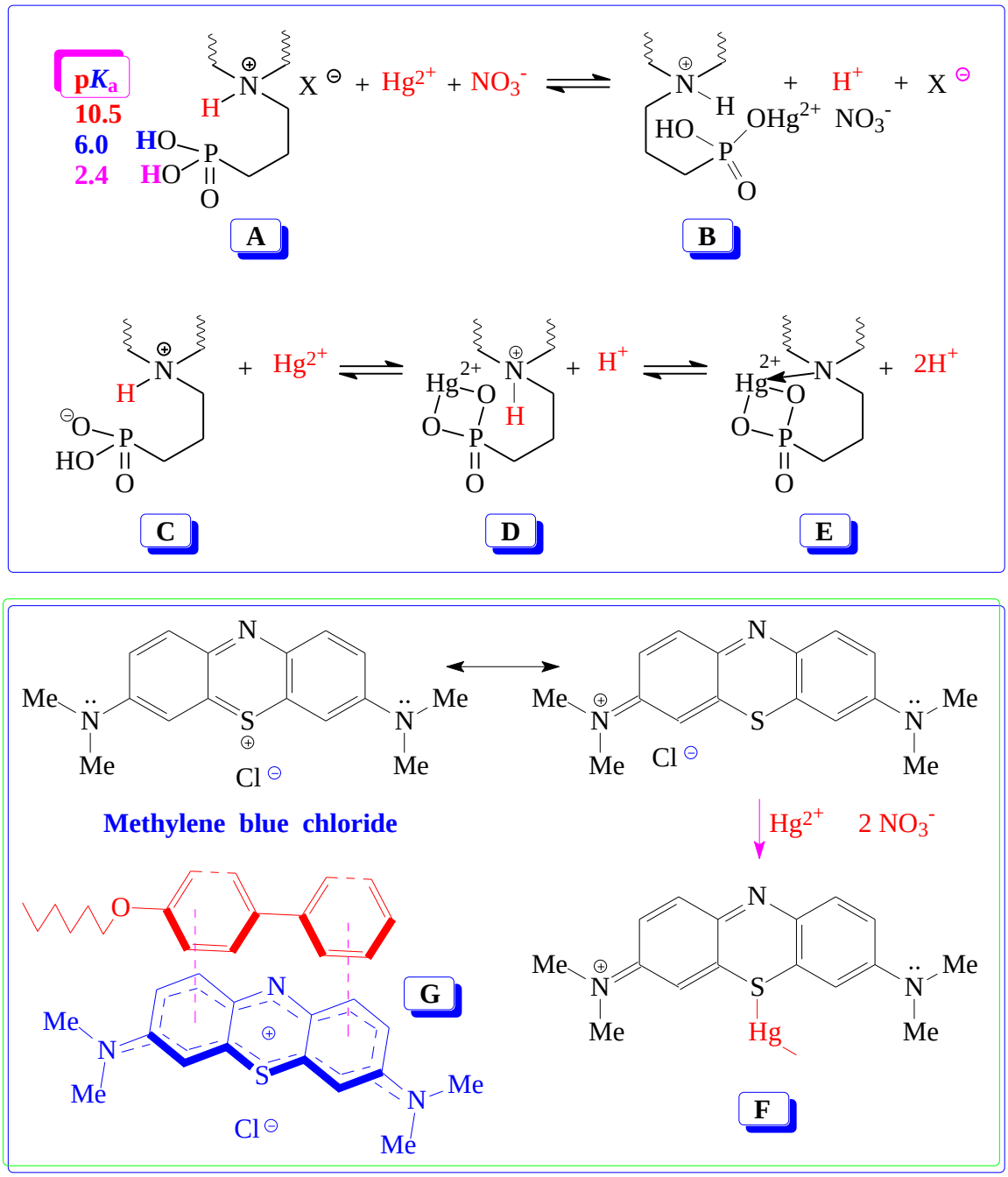

Figure 2.5 Aminopropylphosphonate as a chelating ligand and Hydrophobic interaction between MB and p-phenylphenoxy pendant

2.3.7 Regeneration and Treatment of real wastewater samples

The regeneration tests were achieved by using 0.1 M HCl for Hg(II) and acetone for methylene blue. The polymer has advantageous properties such as active sites, high adsorption capacity, high reusability, easy-to-use, and cost-effective. The polymer has demonstrated remarkable efficiency in removing toxic Hg(II) ions and methylene blue from waters even after 3 cycles with ±3% changes. Thus, the results encourage testing the polymer with the real sample. The industrial wastewater samples were used to study the effect of real water matrix and to evaluate practical application of the polymer. The sample was spiked with 10000 (μg L^{-1}) Hg(II) and 1 μM dye, and then treated with the polymer under the optimum conditions. The dye concentration was analyzed using the UV-vis spectrophotometer. **Table 2.4** presents the analysis of wastewater sample. The % removals are remarkable; the resin captured efficiently not only the metal ions but also As, suggesting its efficiency as an anion exchanger as discussed earlier in the case of NO_3^- (*vide supra*). It is indeed pleasing to see the complete simultaneous removal of the dye. This indicates the high efficiency and capability of the resin to be regarded as a potential adsorbent for high efficient and renewable adsorbent for Hg(II) ions from aqueous solutions.

Table 2.4 Comparison of Hg(II) and dye concentrations in wastewater sample before and after the treatment with the polymer

Metal	Original sample ($\mu g\ L^{-1}$)	Original sample *spiked* with 10000 ($\mu g\ L^{-1}$) Hg(II) and 1 µM dye; then treated with the polymer	Removal (%)
Hg	10.85	88.23	99
Pb	14.45	0.56	96
Co	0.37	0.15	60
Cu	758.0	312.2	59
As	6.52	1.25	81
Mo	29.39	1.98	93
Cd	3.18	<MDL	≈100
Dye	1 µM	<MDL	≈100

MDL: the method detection limit

2.4 Conclusions

The present study was focused on the synthesis, chemical, morphological and thermal characterization of a new novel polymer. We reported on the investigation of adsorption potential of newly developed polymer in the single and simultaneous exclusion of Hg(II) ions and methylene blue from aqueous solutions. The resin showed good adsorption performance with high Langmuir monolayer adsorption capacity at pH 5 at 24 °C. The kinetic assessments revealed that the adsorption process of Hg(II) and methylene blue onto the polymer was progressed via the second-order kinetic mechanism with an R^2 value of >0.99 for all studied concentrations. The initial concentration, temperature, and pH as well as the surface-active sites all contribute to adsorption efficiency. The regeneration tests were achieved by using 0.1 M HCl for Hg(II) and acetone for methylene blue. In addition to being cost-effective, the resin has advantageous properties such as active sites, high adsorption capacity, high reusability, easy-to-use, and cost-effective. The polymer has demonstrated remarkable efficiency in simultaneous removal of toxic Hg(II) ions and methylene blue from aqueous systems.

2.5 References

[1] A. R. A. Syukor, S. Sulaiman, M. N. I. Siddique, A. W. Zularisam, and M. I. M. Said, “Integration of phytogreen for heavy metal removal from wastewater,” J. Clean. Prod., vol. 112, pp. 3124–3131, 2016.

[2] X. Liu and D. J. Lee, “Thermodynamic parameters for adsorption equilibrium of heavy metals and dyes from wastewaters,” Bioresour. Technol., vol. 160, pp. 24–31, 2014.

[3] M. Rahimdokht, E. Pajootan, M. Arami, “Central composite methodology for methylene blue removal by Elaeagnus angustifolia as a novel biosorbent,” J. Environ. Chem. Eng., vol. 4, no. 2, pp. 1407–1416, 2016.

[4] T.A. Saleh, Mercury sorption by silica/carbon nanotubes and silica/activated carbon: a comparison study, Journal of Water Supply: Research and Technology-Aqua 64,8 (2015), 892-903

[5] J. Singh, K. J. Reddy, Y.-Y. Chang, S.-H. Kang, and J.-K. Yang, “A novel reutilization method for automobile shredder residue as an adsorbent for the removal of methylene blue: Mechanisms and heavy metal recovery using an ultrasonically assisted acid,” Process Saf. Environ. Prot., vol. 99, pp. 88–97, 2016.

[6] X. Tao, K. Li, H. Yan, H. Yang, and A. Li, “Simultaneous removal of acid green 25 and mercury ions from aqueous solutions using glutamine modified chitosan magnetic composite microspheres,” Environ. Pollut., vol. 209, pp. 21–29, 2016.

[7] M. Visa and A. M. Chelaru, “Hydrothermally modified fly ash for heavy metals and dyes removal in advanced wastewater treatment,” Appl. Surf. Sci., vol. 303, pp. 14–22, 2014.

[8] D. Zheng, et al. “Facile synthesis of magnetic resorcinol-formaldehyde (RF) coated carbon nanotubes for methylene blue removal,” RSC Adv., vol. 6, pp. 11973–11979, 2016.

[9] G. Li, et al., “Effect of a magnetic field on the adsorptive removal of methylene blue onto wheat straw biochar,” Bioresour. Technol., vol. 206, pp. 16–22, 2016.

[10] W. Yuan, et al. “Journal of Colloid and Interface Science In situ hydrothermal synthesis of a novel hierarchically porous TS-1 / modified-diatomite composite for methylene blue (MB) removal by the synergistic effect of adsorption and photocatalysis,” J. Colloid Interface Sci., vol. 462, pp. 191–199, 2016.

[11] A. P. Heitmann, et al., “Nanostructured niobium oxyhydroxide dispersed Poly (3-hydroxybutyrate) (PHB) films: Highly efficient photocatalysts for degradation methylene blue dye,” Appl. Catal. B Environ., vol. 189, pp. 141–150, 2016.

[12] TA Saleh, A Sarı, M Tuzen, Optimization of parameters with experimental design for the adsorption of mercury using polyethylenimine modified-activated carbon, Journal of Environmental Chemical Engineering 2017, 5 (1), 1079-1088

[13] TA Saleh, AM Muhammad, B Tawabini, SA Ali, Aminomethylphosphonate Chelating Ligand and Octadecyl Alkyl Chain in a Resin for Simultaneous Removal of Co (II) Ions and Organic Contaminants, Journal of Chemical & Engineering Data 2016, 61 (9), 3377-3385

[14] TA Saleh, AM Muhammad, SA Ali, Synthesis of hydrophobic cross-linked polyzwitterionic acid for simultaneous sorption of Eriochrome black T and chromium ions from binary hazardous waters, Journal of colloid and interface science 2016, 468, 324-333

[15] TA Saleh, Isotherm, kinetic, and thermodynamic studies on Hg (II) adsorption from aqueous solution by silica-multiwall carbon nanotubes, Environmental Science and Pollution Research, 2015. 22 (21): 16721-16731.

[16] S. A. Ali,.; Ahmed, S. Z.; Hamad, Z. Cyclopolymerization studies of diallyl- and tetraallylpiperazinium salts. J. Appl. Polym. Sci. 1996, 61, 1077-1085.

[17] A. A. Shaikh, Izzat W. Kazi, Nisar Ullah, A New Chelating Ion-Exchange Resin Synthesized via Cyclopolymerization Protocol and its Uptake Performance for Metal Ions, Ind. Eng. Chem. Res., 2015, 54 (40), pp 9689–9698

[18] A. Yamaguchi, A. Yoshizawa, Phase Transition Behaviour of Amphiphilic Supermolecules Possessing a Semiperfluorinated Alkyl Chain, Mol. Cryst. Liq. Cryst., 479, 181–189, 2007

[19] S. Kudaibergenov, W. Jaeger, A. Laschewsky, Polymeric Betaines: Synthesis, Characterization and Application, Adv. Polym. Sci. 201 (2006) 157-224.

[20] G.B. Butler, Cyclopolymerization and cyclocopolymerization, Marcel Dekker, New York, 1992.

[21] S. A. Ali, O. C. S. Al-Hamouz, "Comparative solution properties of cyclocopolymers having cationic, anionic, zwitterionic and zwitterionic/anionic backbones of similar degree of polymerization", Polymer 53 (2012) 3368-3377.

[22] S. A. Haladu, S. A. Ali, A pH-Responsive Cyclopolymer having phospho- and sulfopropyl pendents in the same repeating unit: Synthesis, Characterization and its application as an antiscalant, J. Polym. Sci., Part A: Polym. Chem. 51, 2013, 5130–5142.

[23] S. Martínez-Tapia, H., et al., Synthesis and Structure of Na2[(HO3PCH2)3NH]1.5H2O: The First Alkaline Triphosphonate. Journal of Solid State Chemistry, 2000. 151(1): p. 122-129.

[24] S. Lagergren, About the theory of so-called adsorption of solution substances, kunglia srenska vertens Ka psakademiens Handlingar. 1898. 24: p. 1-39.

[25] Y.-S. Ho,, Review of second-order models for adsorption systems. Journal of hazardous materials, 2006. 136(3): p. 681-689.

[26] I. Langmuir,, The adsorption of gases on plane surfaces of glass, mica and platinum. J. Am. Chem. Soc, 1918. 40: p. 1362-1403.

[27] T.W. Weber, and R.K. Chakravorti, Pore and solid diffusion models for fixed-bed adsorbers. AIChE Journal, 1974. 20(2): p. 228-238.

[28] T.A. Saleh, 2015, Mercury sorption by silica/carbon nanotubes and silica/activated carbon: a comparison study, Journal of Water Supply: Research and Technology-Aqua 64 (8), 892-903

[29] P. Sivakumar, and P. N. Palanisamy, “Adsorption studies of basic red 29 by a non conventional activated carbon prepared from euphorbia antiquorum L”, Int. J. Chem. Tech. Res, Vol.1, no 3, pp 502-510, 2009.

[30] K.K.H. Choy, G.Mckay and J.F. Porter, “Sorption of acidic dyes from effluents using activated carbons”, Resource. Conserv. Recycling, Vol.27, pp 57-71, 1999.

[31] E.A. Kim, Angelia L. Seyfferth, Scott Fendorf, Richard G. Luthy, Immobilization of Hg(II) in water with polysulfide-rubber (PSR) polymer-coated activated carbon, water research 45 (2011) 453-460

[32] J. Wang,, Deng, B., Wang, X., Zheng, J., 2009. Adsorption of aqueous Hg(II) by sulfur-impregnated activated carbon. Environ. Eng. Sci. 26 (12), 1693-1699.

[33] J.B. Lambert,, Shurvell, H.F., Lightner, D.A., Cooks, R.G., 1987. Introduction to Organic Spectroscopy. In: Group Frequencies Infrared and Raman, vol. 9. Macmillan Publishing Company, New York.

[34] S.A. Ali, N.Y. Abu-Thabit, H.A. Al-Muallem, Synthesis and solution properties of a pH-responsive cyclopolymer of zwitterionic ethyl 3-(N,N-diallylammonio) propanephosphonate, J. Polym. Sc., Part A: Polym. chem. 48 (2010) 5693-5703.

[35] L.D. Freedman, G.O. Doak, The Preparation and Properties of Phosphonic Acids, Chem. Rev. 57(1957) 479–523.

[36] S. K. Sahni,; Bennekom, R. V.; Reedijk, J. A spectral study of transition-metal complexes on a chelating ion-exchange resin containing aminophosphonic acid groups. Polyhedron 1985, 4, 1643–1658.

[37] D. Kolodynska,; Hubicki, Z.; Pasieczna-Patkowska, S. FT-IR/PAS studies of Cu(II)EDTA complexes sorption on the chelating ion exchangers. Acta Phys. Pol., A 2009, 116, 340–343.

[38] D. Kołodynska,; Hubicki, Z.; Geca, M. Application of a New-Generation Complexing Agent in Removal of Heavy Metal Ions from Aqueous Solutions. Ind. Eng. Chem. Res. 2008, 47, 3192-3199.

[39] C. H. Langford,; Langford, P. O. Sulfone Ligands in Cobalt(II) Complexes. Inorg. Chem., 1962, 1, 184–185.

[40] L-J. Li, et al. Synthesis and Characterization of Two Pb(II) Complexes of 2,2′-dihydroxy, Dimethoxy-1,1′-binaphthyl-3,3′-dicarboxylic Acid. Mol. Cryst. Liq. Cryst. 2014, 593, 187-200.

[41] Y. Kawamura,; Mitsuhashi, M.; Tanibe, H.; Yoshida, H. Adsorption of metal ions on polyaminated highly porous chitosan chelating resin. Ind. Eng. Chem. Res. 1993, 32, 386−391.

[42] M. M. Raj, A. Dharmaraja, S. J. Kavitha, K. Panchanatheswaran, D. E. Lynch, Mercury(II)–methylene blue interactions: Complexation and metallate formation, Inorg. Chim.Acta 360 (2007) 1799–1808

[43] X. He, et al. Adsorption and Desorption of Methylene Blue on Porous Carbon Monoliths and Nanocrystalline Cellulose, *ACS Appl. Mater. Interfaces*, 2013, 5, 8796–8804

CHAPTER 3

SIMULTANEOUS TRAPPING OF CR(III) AND ORGANIC DYES BY A PH-RESPONSIVE RESIN CONTAINING ZWITTERIONIC AMINOMETHYLPHOPHONATE LIGANDS AND HYDROPHOBIC PENDANTS

3.1 Introduction

The presence and toxic effect of pollutants in water bodies have been identified as a global challenge [1, 2]. The presence of pollutants in the environment can be attributed to both natural and anthropogenic sources [3]. Heavy metal ions (HMI) are non-biodegradable pollutants accumulated in groundwater and on the soil surface as a waste of some industrial processes such as mining, painting, and anti-corrosive coating. Heavy metal ions over the normal limit can cause a variety of diseases, which include loss of memory, kidney and renal problems, diarhea, as well as reproductive disorders. The presence of the metal contaminants may lead to neurological disorder, damage to both respiratory and cardiovascular organs, skin diseases and cancer [4]. The contaminants are also known to biomagnify in organisms thereby increasing their toxic effects as they move up the food chain [5, 6]. According to the Environmental Protection Agency, the maximum level of the contaminant of chromium, one of the most dangerous metal ions, in drinking water is 0.1 $mg \bullet L^{-1}$.

To overcome the problems caused by pollutants, more efforts are required to minimize their impact on the environment. Different removal methods have been adopted in the treatment of Cr(III)-contaminated waters that include nanofiltration [7], lime-softening [8],

adsorption, reverse osmosis, coagulation [9], electrocoagulation [10], ion exchange, chemical precipitation, etc [11]. Adsorption is considered a promising method relying on the efficiency of the sorbent materials. The use of water-insoluble/swellable solid adsorbents has been found to be efficient because of their ease of phase separation and high enrichment efficiency [12-13].

Designing an appropriate and efficient adsorbent for specific pollutants is the key step for a successful adsorption process. For metal removal from wastewater, conventional adsorbents like clay activated carbon and nanomaterials are used. Inexpensive biodegradable natural polymers such as cellulose, chitosan and starch are also used because of their abundance, high efficiency, non-toxic nature, and eco-friendliness. At industrial application, there is a need for more advanced properties of an adsorbent such as fast adsorption kinetics, high capacity, and temperature stability. Polymer materials could be used as candidates to fulfill such industrial requirements. Zwitterionic cross-linked organic and inorganic hybrid polymer drew attention because they can remove HMI by electrostatic effects [12, 13].

The production of total dyes exceeds the 700,000 tons per year [14]; the discharge of ≈2% of the total production in wastewater poses a serious environmental challenge owing to their high toxicity and carcinogenic and mutagenic characteristics [15]. Solid adsorbents, having advantages of low cost and simple operation without causing secondary pollution, are widely used to remove dyes from wastewater [16,17]. However, adsorbents like activated carbon, silica, zeolite, and chitosan, etc., have relatively low adsorption capacity owing to their weak affinity to HMI and dyes [18- 21]. Graphene oxide (GO), as well as its decorated derivatives, have got considerable attention for environmental applications because of their enormous surface area [18, 22-24]. However, GO has its inherent problem of aggregation

or agglomeration in aqueous solution owing to the strong □–□ interactions between graphitic layers; as a result, a low effective surface area put a limitation for wide application as adsorption materials [18, 25].

Thus, there is tremendous scope to develop new materials with high affinity to both HMI and dyes. Aminomethylphosphonate (□$NH^+CH_2PO_3H$□) as a chelating ligand, has etched a place of distinction in the removal of heavy metal ions [26-30]. Being the pH-responsive zwitterionic motifs, the ligand may be tuned to trap metal cations, toxic anions (like AsO_4^-) as well as organic dyes of both algebraic signs. The affinity towards dyes may as well be augmented by the presence of hydrophobic aromatics capable of □-□ interactions thereby leading to their association and entrapment. The goal of the work is to synthesize a novel functionalized resin with hydrophilic motifs of aminomethylphosphonate and hydrophobic pendants of 4-(6-hexyloxy)biphenyl as a sorbent for the removal of Cr(III) as a model case as well as several organic dyes from aqueous solutions (Scheme 1).

3.2 Experimental

3.2.1 Chemicals and Materials

Stock solutions of analytical grade Cr(III) nitrate (1000 mg/L), HNO_3, HCl, and NaOH were purchased from Sigma-Aldrich, USA. The standard stock solution was diluted to the predetermined concentrations for the adsorption tests. 2,2′-Azoisobutyronitrile (AIBN) (from Fluka AG) was crystallized from a chloroform-ethanol mixture. Dimethylsulfoxide (DMSO) was purified by drying (CaH_2) and distilling at 64-65°C (4 mmHg). Monomer **1** (≈100% purity, was prepared by a modified procedure which avoided silica gel

chromatography) [31]. Cross-linker **3** [32] was synthesized using a literature procedure. 4-(6-Bromohexyloxy)biphenyl: Ph-PhO$(CH_2)_6$Br were prepared as described [33]. Chromium standard solution (1000 ppm) was used to prepare the diluted solutions of the required concentrations. Millipore water (18.2 MΩ·cm) was used for the adsorption study.

3.2.2 Characterization Techniques and procedures

Perkin Elmer Elemental Analyzer Series 11 Model 2400 (Waltham, Massachusetts, USA) was used for elemental analysis, while IR analyses were performed on a Thermo scientific FTIR spectrometer (Nicolet 6700, Thermo Electron Corporation, Madison, WI, USA) with deuterated triglycine sulfate detector. The background correction of the spectra was performed by 16 scans with a resolution of 2 cm^{-1}. NMR spectra were collected in a JEOL LA 500 MHz spectrometers using $CDCl_3$ with tetramethylsilane (TMS) as internal standard (^1H signal at δ 0 ppm), while in D_2O, residual proton HOD signal at δ4.65 ppm and dioxane ^{13}C signal at 67.4 ppm were taken as internal and external standards, respectively.–The resin's morphology was examined by Scanning electron microscope (SEM). Energy-dispersive X-ray spectroscopy (EDX) fitted with an X-Max detector was used to get the elemental spectra of the resin.

The thermal stability of the resin was evaluated by Thermogravimetric analysis (TGA) with an SDT Q600 thermal analyzer from TA instruments, USA. The temperature was raised at a rate of 10°C/min over a temperature range 20–800°C using Platinum/Platinum–Rhodium (Type R) thermocouples under air flowing at a rate of 100 mL/min. A thermogravimetric and differential scanning calorimetry (TGA-DSC) thermal analysis was performed on the sample to understand the thermal stability of the adsorbent.

The BET surface area, pore size, and volumes of the samples were measured on micromeritics Tristar surface area and porosimetry analyzer (Micromeritics, USA) using liquid N_2 adsorption-desorption at -196 ^oC by the methods of Brunauer-Emmett-Teller (BET) and Barrett-Joyner-Halenda (BJH). Prior to measurement, the samples were degassed at 150 ^oC for 3 h to remove the presence of impurities or moisture. The contribution of micropore and mesopores was computed from the *t*-plot method according to Lippens and de Boer. Atomic Absorption spectroscopy (Thermo Scientific iCE 3000) was employed to monitor the concentration of Cr(III). The concentration of the tested dyes was monitored in a UV-vis spectrophotometer using optical quartz cuvettes. Inductively Coupled Plasma – Mass Spectrometer (ICP-MS) technique was employed to analyze the real wastewater samples.

3.2.3 Synthesis of monomers 2

A solution of 4-(6-bromohexyloxy)biphenyl Ph-PhO$(CH_2)_6$Br (3.33 g, 10.0 mmol) and diallylamine (4.9 g, 50 mmol) in toluene (5 mL) was heated under N_2 at 100 °C for 24 h. The reaction mixture, taken up in ether (50 mL), was washed with 5% NaOH solution (20 mL). The organic extract was dried (Na_2SO_4), concentrated and purified by chromatography over silica gel using ether/hexane mixture as eluent to obtain 4-(6-hexyloxybiphenyl)diallylamine (3.0 g, 86%) which on treatment with dry HCl in ether afforded monomer **2** as a white solid in quantitative yield. M.p. 108-110 °C; (Found: C, 74.4; H, 8.4; N, 3.6%. $C_{24}H_{32}ClNO$ requires C, 74.68; H, 8.36; N, 3.63). $\nu_{max.}$ (KBr) 3478, 3402, 3327, 3224, 3084, 3029, 2946, 2867, 1653, 1623, 1606, 1518, 1488, 1392, 1289, 1270, 1244, 1194, 1176, 1116, 1043, 1021, 997, 944, 848, 821, 772, 720, and 701 cm^{-1}; δ_H

($CDCl_3$) 1.42 (2H, quint, *J* 7.3 Hz), 1.53 (2H, quint, *J* 7.3 Hz), 1.80 (2H, quint, *J* 6.7 Hz), 1.89 (2H, m), 2.96 (2H, m), 3.63 (4H, m), 3.98 (2H, t, *J* 6.4 Hz), 5.52 (4H, m), 6.14 (2H, m), 6.95 (2H, d, *J* 8.6 Hz), 7.29 (1H, t, *J* 8.3 Hz), 7.41 (2H, t, *J* 7.6 Hz), 7.52 (2H, d, *J* 8.8 Hz), 7.54 (2H, d, *J* 8.3 Hz), 12.48 (1H, s).

3.2.4 Resin synthesis Quadripolymerization of monomers 1, 2, cross-linker 3 and SO_2 to hydrophobic cross-linked polyzwitterionic acid (HCPZA) 4

Sulfur dioxide was absorbed (1.96 g, 30.6 mmol) to a solution of **1** (4.56 g, 20 mmol), **2** (2.00 g, 5.0 mmol), and **3** (0.890 g, 2.78 mmol) in DMSO (16 g) in a RB flask (50 cm^3). Initiator AIBN (250 mg) was added under N_2, and then the mixture was stirred in the closed flask at 65 ºC. Within 1 h, the mixture became an immovable transparent gel, and the polymerization was continued at 65 ºC for 24 h. The flask was cooled and opened every 8 h to release N_2 produced during the decomposition of the initiator. Finally, the white resin was washed with liberal excess of water and acetone. Resin HCPZA **4** was dried under vacuum at 65ºC for 6 h (7.8 g, 83%). The resin was found to have: C, 39.1; H, 6.3; N, 4.9; S, 11.2. HCPZA **4** containing **1** (72.0 mol%), **2** (18.0 mol%), **3** (10.0 mol%) and SO_2 (100 mol%) requires C, 39.63; H, 5.98; N, 5.12; S, 11.72%.

3.2.5 Conversion of HCPZA 4 to hydrophobic cross-linked dianionic polyelectrolyte (HCDAPE) 5

Resin **4** (0.50 g, 1.6 mmol) was treated with NaOH (0.18 g, 4.5 mmol) in water (5 mL); after 1 h at room temperature, a mixture of methanol (20 mL) containing NaOH (0.18 g, 4.5 mmol) was added to the gel. After filtering and washing with methanol, the resultant HCDAPE **5** was dried under vacuum for 6 h at 65 °C (0.51 g, 90%). The resin was found to have: C, 37.2; H, 5.2; N, 4.5; S, 10.3. HCDAPE **5** containing repeating units derived from **7** (72.0 mol%), **6** (18.0 mol%), **8** (10.0 mol%) and SO_2 (100 mol%) requires C, 37.52; H, 5.09; N, 4.64; S, 10.63%. $\nu_{max.}$ (KBr) 3420 (v broad), 2093, 1657, 1520, 1486, 1418, 1299, 1123, 1066, 976, 845, 766, and 557 cm^{-1}.

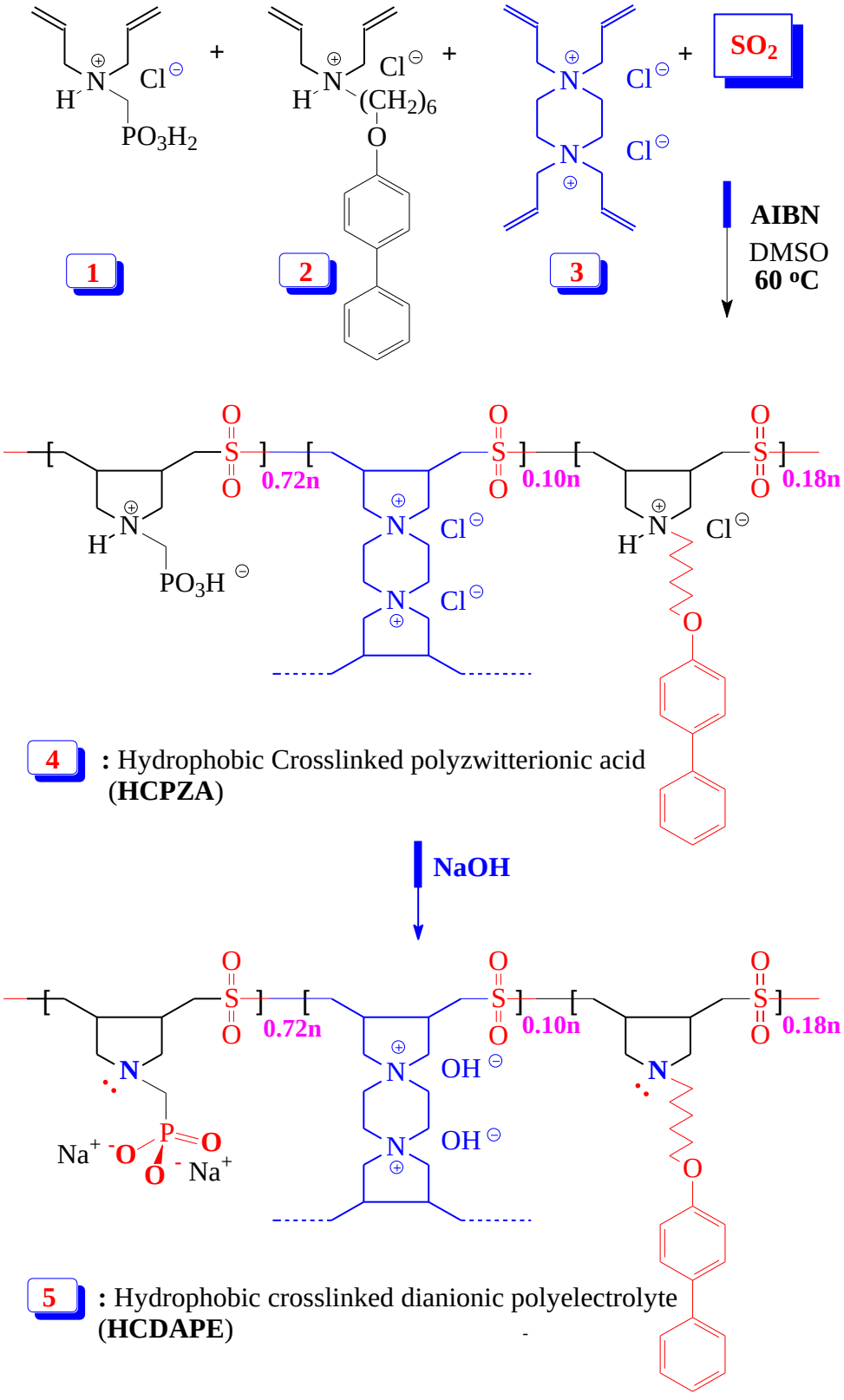

Figure 3.1 Synthetic Scheme

3.2.6 Swelling coefficient

The swelling coefficient is the ratio of the wet volume of the resin to the dry volume. The swelling coefficient was evaluated as follows: resins were properly crushed and a 20- to 30-mesh fraction was used. To a certain volume of the dry resin in a burette, sufficient water was added to cover its level; the equilibrated volume of the wet sample was measured and compared with the volume of the dry resin.

3.2.7 Batch Experiments

Adsorption efficiency was assessed by the batch experiments carried out as follows: 5, 10, and 20 mg of the resin **4** was mixed in aqueous Cr (III) solution and stirred at various periods during 120 min at 298 K. The initial concentration of Cr(III) was varied. The Cr(III) solution then filtered and analyzed by AAS to quantify the Cr (III) ion uptake. To gain thermodynamic and kinetic data, batch experiments were performed at temperatures of 298, 318 and 338 K.

The binary system experiments were performed using 30 mg of resin **4**, in aqueous solution (20 mL) having 1 ppm concentration of each of Cr(III) and dyes. The resultant solutions were analyzed by ICP for Cr (III) ions, while UV-Vis spectrometer was used for the analysis of dye compounds: methyl orange, eriochrome black T, rhodamine B, methyl red and methylene blue.

The kinetic studies were performed under the optimized conditions of shaking speed (150 rpm) and pH (5). Containers containing a mixture of the adsorbates and resin were agitated in a shaker at 25 ^{o}C and aliquots were collected at time intervals up to 120 min. After the equilibrium, final methyl orange, Eriochrome black T, rhodamine B, methyl red and

methylene blue concentrations were analyzed using UV–Vis spectrophotometer and the Cr(III) concentration was monitored by flame atomic spectroscopy.

3.2.8 Data Analysis

The percent removal of Cr(III) at the equilibrium was calculated by the equation:

$$\%\ Removal = \frac{C_\circ - C_e}{C_\circ} \times 100 \qquad (1)$$

Adsorption capacities were calculated using the equations:

$$q_e = (C_o - C_e) \times \frac{V}{m} \qquad (2)$$

and

$$q_t = (C_o - C_t) \times \frac{V}{m} \qquad (3)$$

In equation (2), the adsorption capacity q_e (mg g^{-1}) at equilibrium is the amount of Cr(III) adsorbed per gram of the resin. Meanwhile, in equation (3), the adsorption capacity q_t (mg g^{-1}) is the adsorbed Cr (III) (mg) per gram of **4** at time *t*. C_o, C_e and C_t are the initial concentration (mg L^{-1}) of Cr(III) and its concentrations at the equilibrium and at time *t*, respectively. *V* (L) and *m* (g) stand for the solution volume and the mass of the resin, respectively.

3.2.9 Adsorption/Desorption experiment

After stirring resin **4** (20 mg) in 1.0 ppm Cr(III) solution (40 mL) at pH 5 for 24 h and then centrifuging, the q_e value was determined by AAS to quantify the Cr(III) ion left in the supernatant liquid. For the desorption process, the metal ions- loaded resin in the centrifuge tube was washed with the pH 5 buffer solution, then treated with 0.1 M HNO_3 (20 mL) at room temperature for 6 h. The concentrations of the desorbed metal ions were determined and used to calculate the efficiency of desorption process. The resin left in the centrifuge

tube was washed with deionized water; as described above, the adsorption/desorption procedure was repeated three times. It is worth mentioning that the procedure ensured the use of a fixed amount of the same resin three times. Centrifugation ensured no loss of the resin as it may happen in the usual filtration procedure.

Similar adsorption/desorption experiments were carried out for a Cr(III)-Eriochrome Black Tea binary system. As described before, the adsorption experiment for binary systems were performed using 30 mg of resin **4** (20 mg) in aqueous solution (40 mL) having 1 ppm concentration of each of Cr(III) and Eriochrome Black Tea at pH 5. After centrifuging, the supernatant solutions were analyzed by ICP for Cr (III) ions, while UV-Vis spectrometer was used for the analysis of the dye. The regeneration tests were conducted by washing the loaded resin with acetone to remove Eriochrome Black Tea and, as before, by treating with 0.1 M HNO_3 for the removal of Cr(III).

3.3 Results and discussion

3.3.1 Synthesis and characterization

Cyclopolymerization protocol [34, 35] was exploited in the AIBN-initiated quadripolymerization of hydrophilic monomer **1**, hydrophobic monomer **2** and cross-linker **3**, along with SO_2 as the fourth alternating monomer to obtain hydrophobic cross-linked polyzwitterionic acid (HCPZA) **4** in 83% yield (**Scheme 1**). During the work up, HCl is eliminated to give the zwitterionic aminophosphonate motifs. The composition of the repeating units in the resin matched with the feed ratio of 0.72 : 0.18 : 0.10 : 1.0 for monomers **1**/**2**/**3**/SO_2 as supported by elemental analysis: This is expected for such a high conversion of the monomers to the resin.

HCPZA **4** upon treatment with NaOH was converted to HCDAPE **5**. Zwitterionic resin **4** and its anionic form **5** were found to have swelling coefficients of 1.8 and 6.3, respectively. The zwitterionic form of a compact coil in **4** is expected to have a lower affinity for adsorption of water, while the anionic form **5** has more expanded conformations owing to the repulsion among negative charges and thus has a greater affinity for solvation. The presence of the hydrophobic units and chelating aminophosphonate ligands in the resin would serve dual purposes: with a single treatment, the removal of organic pollutants and toxic metal ions is anticipated.

The FTIR spectra of the resin and Cr(III)-loaded resin are depicted in **Figure 3.1a.** The asymmetric and symmetric bands of SO_2 appeared at ≈1310 cm^{-1} and ≈1124 cm^{-1}, respectively. The bands at 560 – 600 cm^{-1} and 1000 – 1100 cm^{-1} regions can be assigned to phosphonate groups [36]. Adsorbed water band can be seen at around 3400 cm^{-1}, while the band at 1620 cm^{-1} is assigned to the bending vibration of H_2O. The peak at 1477 cm^{-1} is attributed to the C-N stretching. The absorption band at 1075 and 1190 cm^{-1} were assigned to the ν_s (PO_2) and and ν_{as} (PO_2) of PO_3H^- [31].

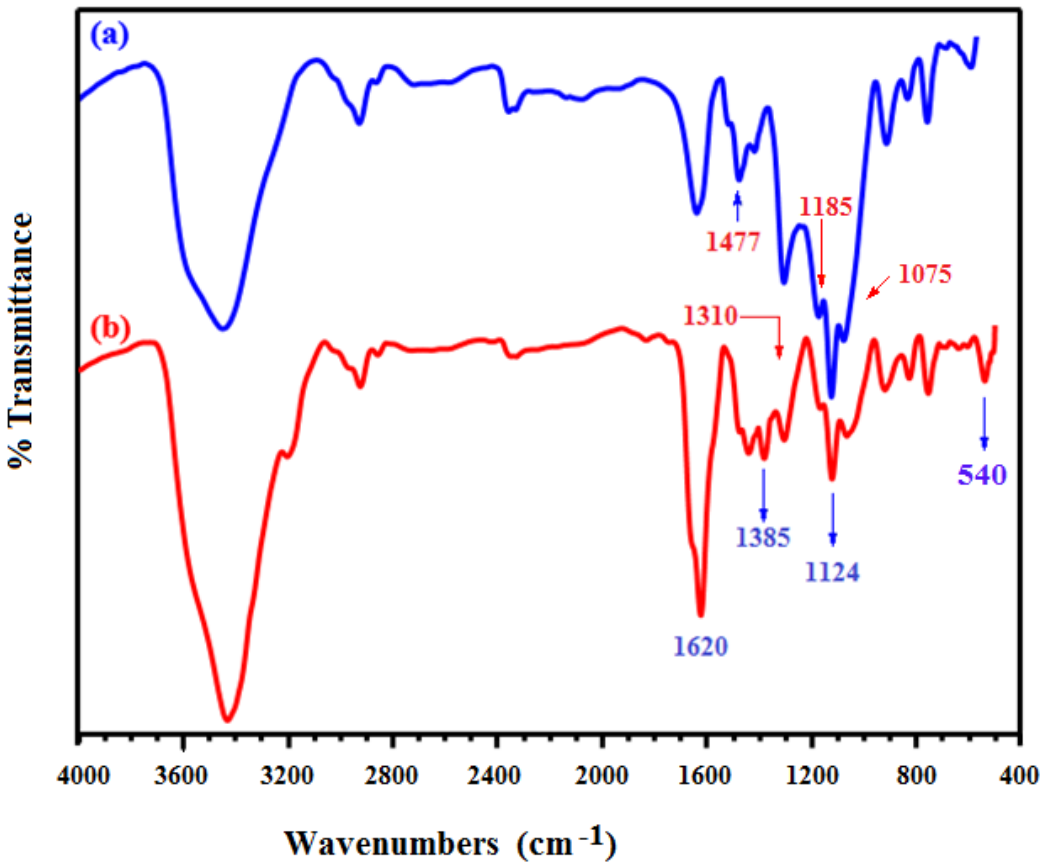

Figure 3.2 IR Spectra of (a) resin 4 and (b) Cr(III)-loaded resin 4

The N_2 adsorption-desorption isotherm displayed by the polymer is given in **Figure 3.2**. It showed a resemblance of Type I isotherm. The presence of hysteresis loop at high relative pressure signified the presence of mesopores while the uptake of nitrogen at low relative pressure confirmed the presence of micropores in the sample. The textural parameters obtained quantitatively were summarized in **Table 3.1** [22]. The resin's surface area of 56 m^2/g is indeed relatively high for an ionic resin [26]. The higher surface area may be attributed to the presence of long hydrophobic tail requiring larger space in the resin matrix.

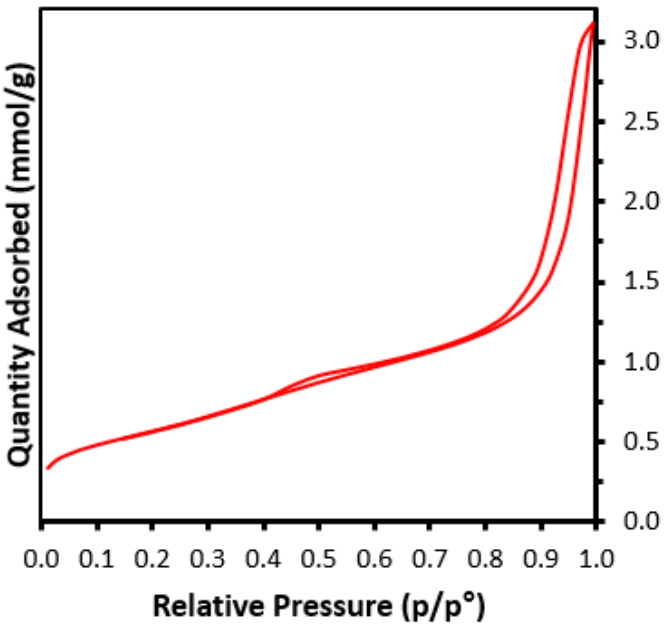

Figure 3.3 BET adsorption-desorption curves of the polymer sample

Table 3.1 Properties of resin 4 obtained from BET surface area analysis

Textural Parameters	Values
BET surface area (S_{BET})	56 m^2g^{-1}
Micropore surface area (S_{micro})	19 m^2g^{-1}
Mesopore surface area (S_{meso})	23 m^2g^{-1}
Total pore volume (V_t),	0.67 cm^3g^{-1}
Micropore volume (V_{micro})	0.08 cm^3g^{-1}
Average pore diameter (APD)	8.3 nm

The TGA curve of the prepared resin, depicted in **Figure 3.3**, revealed two distinct weight loss stages. The first indicates a gradual loss of around 5% upto 225 °C can be assigned to the removal of the trapped moisture and HCl from the material. The second steep loss of ≈ 33% in the range 225- 375 °C is assigned to the loss of phosphonate pendants and SO_2 owing to polymer degradation. The loss thereafter could be attributed to the combustion of functional groups releasing NOx, CO_2, and H_2O gasses [37]. As seen from the **Figure 3.4**, the resin remained stable even at 250 °C.

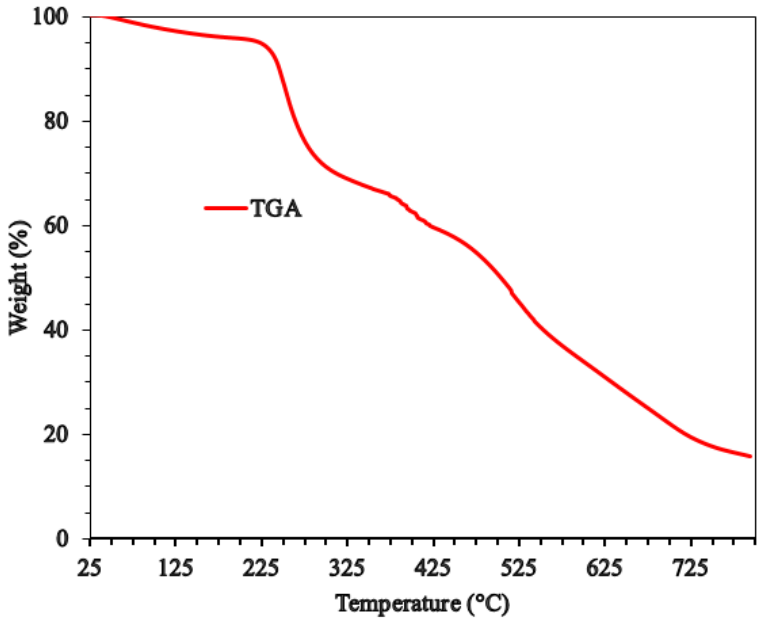

Figure 3.4 TGA curve of resin 4

3.3.2 Evaluation of Adsorption efficiency

3.3.2.1 pH-responsiveness

The dependency of the Cr(III) removal on the pH was studied in the pH range 3-7 using dosages of 5, 10 and 20 mg of the resin in 20 mL aqueous mixture, and the results are depicted in **Figure 3.5.** Solutions of pH > 7 were not examined to avoid the competition between the adsorption and precipitation of the Cr in form of $Cr(OH)_3$. Note that the pH can affect the nature of the chelating motifs in the resin. Adsorption of Cr(III) ions increased with the increase in pH in the range 3 - 7 and the optimum pH value was found to be in the range 5 - 7.

The trend depicted in **Figure 3.5** is explained by considering the surface charge of the resin. The active sites on the resin, play a key role in the removal of Cr(III). At pH > 6, chromium is precipitated as chromium hydroxides [23, 38], while the dominant species in solutions having pH in the range 1 – 6 are $CrOH^{2+}$, $Cr_3(OH)_4^{5+}$ and $Cr_2(OH)_2^{4+}$. The positively charged species are attracted to the negative sites (PO_3H^- and PO_3^{2-}) on the resin. In solution of low pH of 3, the hydronium ions effectively compete with the chromium species for the adsorption sites on the resin, thereby decreasing its adsorption capacity.

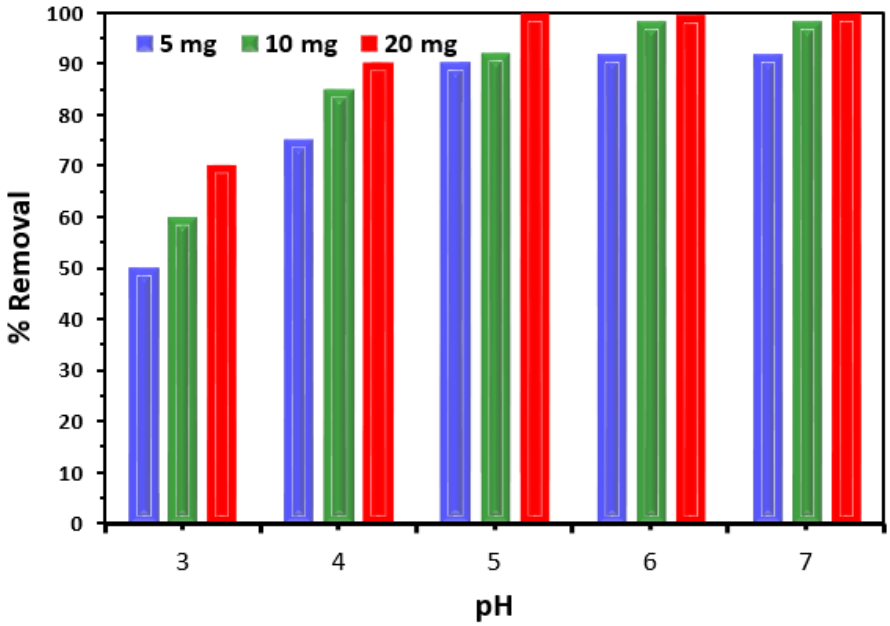

Figure 3.5 Effect of the pH of the solution on percent Cr(III) removal using various dosages of resin 4 in aqueous mixture (20 mL)

3.3.2.2 Contact Time

The batch experiments with initial concentrations of Cr(III) ions; 5, 10, and 20 ppm (20 mL) were carried out at 25 ºC to evaluate the dependency of the adsorption capacity on the contact time. Initially, the rate of adsorption of Cr(III) was fast with steep slopes, while it attained equilibrium adsorption value within 20 min at a resin dosage of 20 mg (**Figure 3.6**).

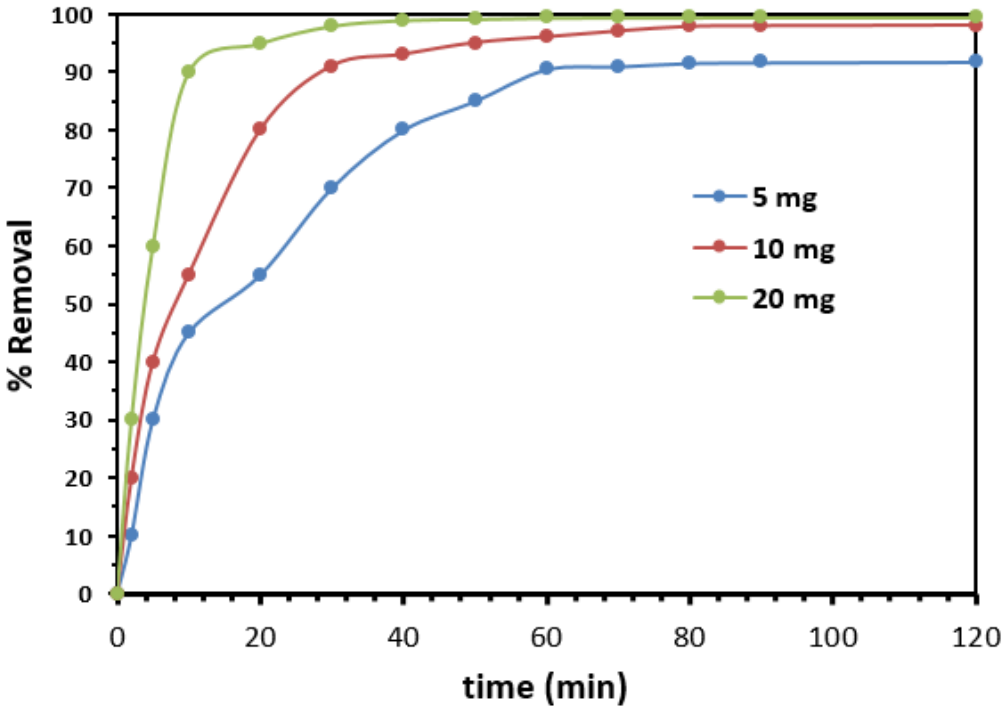

Figure 3.6 Dependency of percent removal of Cr(III) versus contact time with solution containing various dosages of the resin

3.3.3 Kinetics

Lagergren's first and pseudo-second order kinetic models were applied to examine the adsorption mechanisms. For the first order kinetics, linear equation (4) was used [39]:

$$\ln(q_e - q_t) = \ln q_e - k_1 t \qquad (4)$$

where the amounts of Cr(III) (mg/g) adsorbed at *t* and at equilibrium are described by q_t and q_e respectively, while k_1 represents the rate constant. The ln (q_e - q_t) versus *t* plot yielded k_1 and q_e, values (**Figure 3.7a, Table 3.2)**. Disagreement between the experimental ($q_{e,\,exp}$) and calculated value ($q_{e,\,cal}$), and the poor correlation coefficients (R^2) ruled out the adsorption rate obeying the first-order kinetic model. The second-order adsorption rate was obtained using [40]:

$$\frac{dq_t}{dt} = k_2(q_e - q_t)^2 \quad (5)$$

where k_2 represents the rate constant, and q_e and q_t are the respective adsorption capacities at equilibrium and at time *t*.

The pseudo second-order in the linear form is written as follows:

$$\frac{t}{q_t} = \frac{1}{k_2 q_e^2} + \frac{t}{q_e} \quad (6)$$

where k_2 is obtained from t/q_t versus *t* plot (**Figure 3.7b**). The high correlation coefficient values, and agreement between $q_{e,\,cal}$ and the $q_{e,\,exp}$ supported the adsorption process as following the pseudo-second order kinetics model involving predominant chemical interaction between Cr(III) and the chelating ligands (**Table 3.2**).

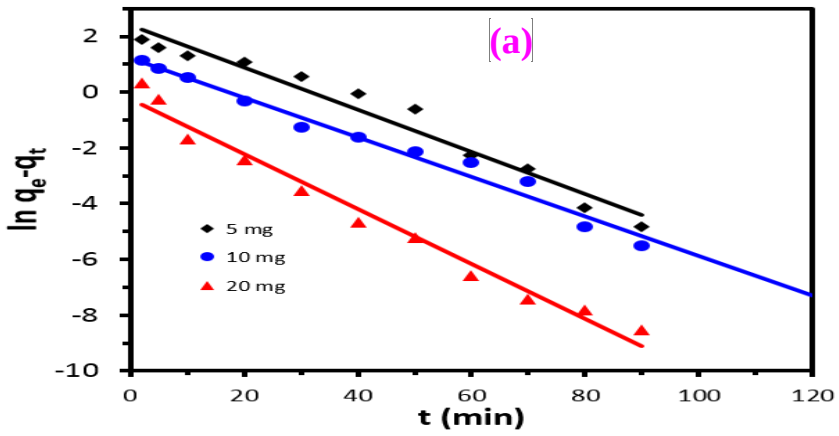

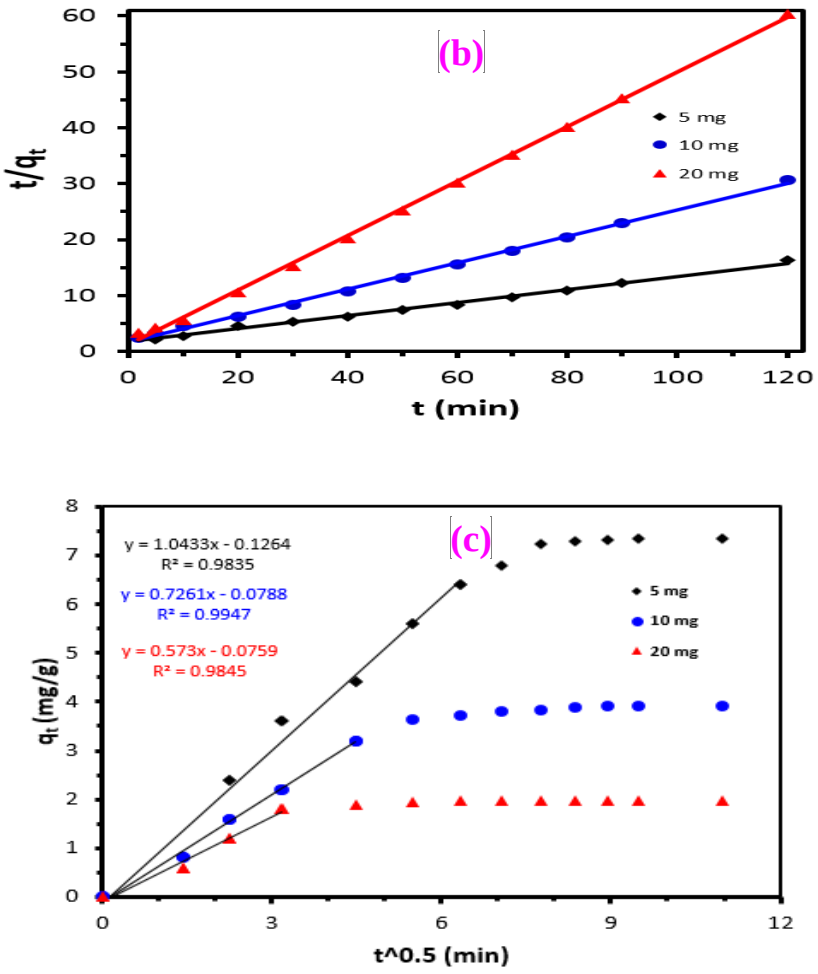

Figure 3.7 (a) Lagergren's first order; (b) Pseudo-second order and (c) Interparticle diffusion model at 298 K

Table 3.2 Kinetic parameters for Cr(III) adsorption on the resin at 298 K

		Lagergren's first order			Pseudo second order			Intraparticle diffusion		
C_i (mg/L)	q_e, exp (mg/g)	k_1 (min^{-1})	q_e, cal (mg/g)	R^2	k_2[a]	q_e, cal (mg/g)	R^2	k_{id}[b]	C (mg/g)	R^2
5	7.34	0.0757	11.0	0.9646	0.00801	8.55	0.9983	0.881	6.87	0.9975
10	3.92	0.0987	3.41	0.9778	0.0294	4.76	0.9988	0.650	5.89	0.9798
20	1.99	0.0711	3.32	0.9796	0.146	2.51	0.9998	0.542	2.91	0.9896

[a] (g/mg•min)

[b] (mg/g•min)

The adsorption results were fitted using Weber's intraparticle diffusion model [41-46]:

$$q_t = k_{id} t^{1/2} + C \quad (7)$$

where a k_{id} (mg/g• $min^{1/2}$) is the constant of intraparticle diffusion rate, C is the intercept (mg/g). The experimental data expressed that initially, the plots of q_t versus $t^{1/2}$ are linear with very good correlation coefficients and passing through the origin (C = ≈ 0), thereby implicating intraparticle diffusion as the rate-limiting step [47,48]. It can be discerned from **Figure 3.7c** that the initial linear portion represents the intraparticle diffusion while the plateau represents the equilibrium.

3.3.4 Adsorption Isotherms

Isotherms models provide fundamental physiochemical data to assess adsorption capacity. Langmuir isotherm, the ideal localized monolayer model, is based on the concept of a homogeneous surface phase. It is used to describe the nature of the process either a physical or chemical, using the equation [42]:

$$\frac{C_e}{q_e} = \frac{1}{k_L q_m} + \frac{C_e}{q_m} \qquad (8)$$

where k_L (L/mg), q_m (mg/g), C_e (mg/L), and q_e (mg/g) represent the affinity of adsorption sites; theoretical monolayer adsorption capacity, the equilibrium concentration of Cr (III) and its amount adsorbed per gram resin, respectively.

The plot of C_e/q_e versus C_e is depicted in **Figure 3.8a**, where the slope and intercept gave the k_L and Langmuir constant q_m, respectively (**Table 3.3**). The separation factor represented by the dimensionless equilibrium parameter R_L is introduced in eq (9) [43]:

$$R_L = \frac{1}{1 + K_L C_o} \qquad (9)$$

where C_o represents the initial solute concentration. The adsorption process becomes unfavourable for R_L>1, linear for R_L = 1, favourable for 0 < R_L< 1, and irreversible when R_L = 0. As shown in **Table 3.3,** the favorabilityof the adsorption is confirmed by the R_L value of 0.57. For the sake of comparison, the maximum adsorption capacity (q_m) of the current resin and some other sorbents reported for the removal of Cr(III) are tabulated in **Table 3.3**; the current resin was found to be more effective than the other sorbents.

Table 3.3 Langmuir, Freundlich and Temkin isotherm parameters for the adsorption of Cr(III) on resin 4

Langmuir				Freundlich				Temkin		
q_m (mg/g)	k_L (L/mg)	R_L	R^2	1/n	n	k_f (mg/g)	R^2	K_T (L/g)	b_T (KJ/mol)	R^2
16	40	0.57	0.9899	0.4756	2.10	24.5	0.9984	1.006	1.29	0.9799

Table 3.4 Comparison between the efficiency of the resin with literature reported adsorbents

Adsorbent	**Initial Conc. (mg/L)**	**pH**	**Cr(III) removal efficiency**	**Loading Capacity (mg/g)**	**Ref.**
Lewatit S: Sulfonic acid group with cross linked polystyrene matrix	52	3.5	99	20	[49]
Amberlite Sulfonic acid group	10	5	87	2.2	[50]
Styrene-DVB	20	5.5	68	2.5	[51]
Coconut shell carbon	50	6	87	20	[52]
Sulfonated styrene/acrylonitrile	30	6	90	7.2	[53]
Sulfonatedpolymethylmethacrylate				9.0	
Polymer	1.0	5.5	99	16	(Current work)

The Freundlich model describes the adsorption characteristics on heterogeneous surfaces where the adsorbed molecules interact among them [44] and is expressed as:

$$q_e = K_f C_e^{\frac{1}{n}} \quad (10)$$

where Freundlich isotherm constant K_F (mg/g) and $1/n$ indicates the adsorption capacity and its intensity, respectively. C_e and q_e describe the concentration (mg/L) of the adsorbate and its amount adsorbed per gram of the adsorbent (mg/g) at equilibrium. The model in linear for is:

$$\ln q_e = \ln K_f + \frac{1}{n} \ln C_e \qquad (11)$$

where K_F and n values as calculated from the ln q_e versus ln C_e plot (**Figure 3.8b**) are included in **Table 3.3.** The n value is used to describe the nature of the adsorption process: 1/n <1 and > 1 imply a normal and a cooperative adsorption, respectively. The 1/n value of ≈ 0.5 in the current work indicates a favorable adsorption process.

The Temkin model considers the interactions between the adsorbent and adsorbate, and it assumes a linear decrease in the adsorption energy as given by [31]:

$$q_e = \frac{RT}{b_T} \ln K_T + \frac{RT}{b_T} \ln C_e \qquad (12)$$

where Temkin isotherm constant b_T describes the heat of sorption (J mol^{-1}), while Temkin isotherm equilibrium binding constant k_T reflects the maximum binding energy (L/g). R and T represent the gas constant (8.314×10^{-3} kJ/mol.K) and temperature (K), respectively. The q_e versus ln C_e plot gave the isotherm constants (**Figure 3.8c**).

As shown in **Table 3.3**, the square of correlation coefficients (R^2) for the Langmuir and Freundlich are found to be excellent and very close, while for the Temkin, the data fit the isotherm reasonably well. The adsorption of Cr(III) by the resin could thus be considered a monolayer adsorption on a heterogeneous surface.

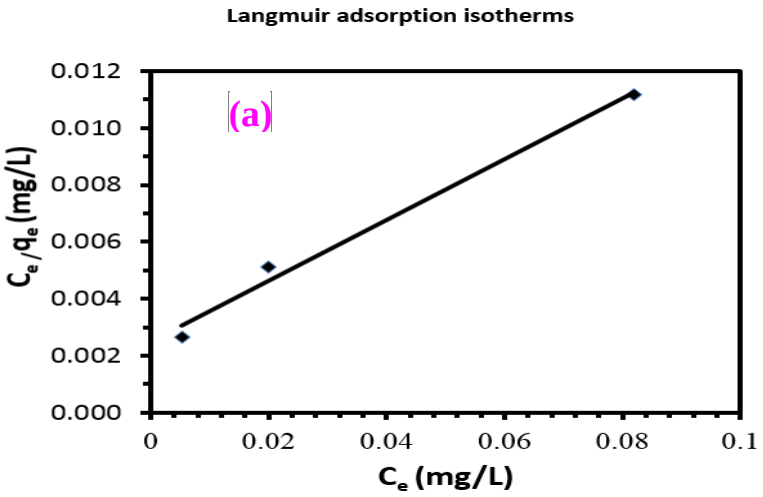
Langmuir adsorption isotherms
(a)
0.012
0.010
0.008
0.006
0.004
0.002
0.000
C_e/q_e (mg/L)
0
0.02
0.04
0.06
0.08
0.1
C_e (mg/L)

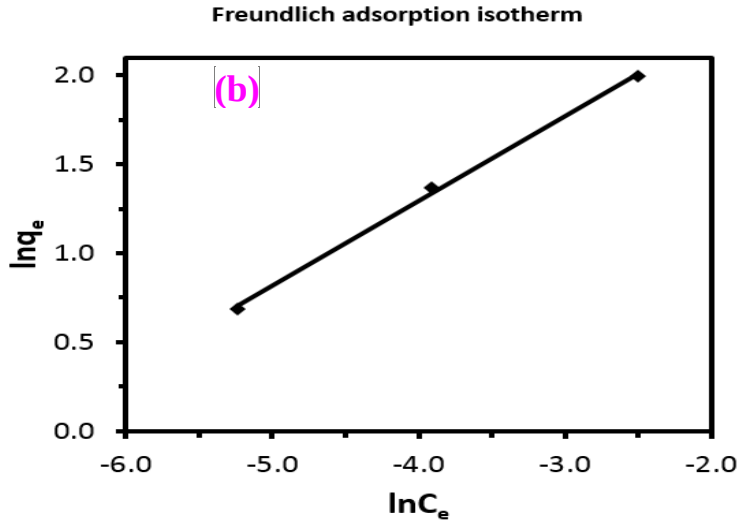
Freundlich adsorption isotherm
(b)
2.0
1.5
1.0
0.5
0.0
$\ln q_e$
-6.0
-5.0
-4.0
-3.0
-2.0
$\ln C_e$

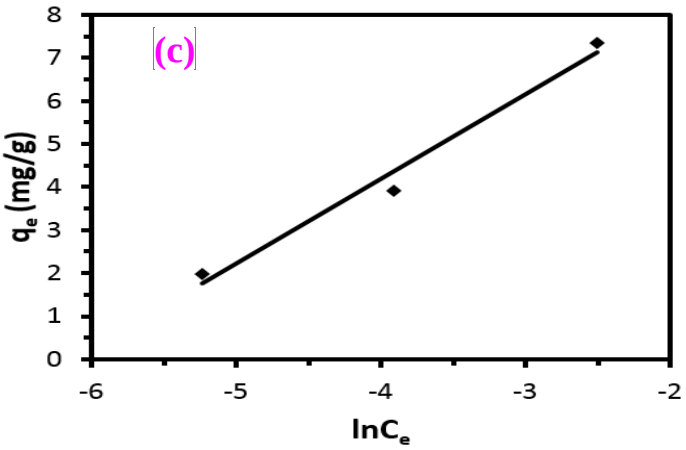

Figure 3.8 (a) Langmuir, (b) Freundlich and (c) Temkin adsorption isotherms for the removal of Cr(III) using the adsorbent

3.3.5 Energy of Activation and Thermodynamics

Using Arrhenius equation [Eq. (13)] and the related plot (Fig. 8a), the activation energy E_a for the adsorption of Cr(III) was determined to be 42.8 kJ/mol which is at the higher end of the range 5 – 40 kJ/mol, considered as the energy requirement for a physisorption process. The adsorption may not be simply an ion exchange process, in addition, it may involve chemical exchange involving chelation.

$$\log k_2 = -\frac{E_a}{2.303\,RT} + \text{constant} \qquad (13)$$

The thermodynamic parameters ΔG^o, ΔH^o and ΔS^o are used to describe the adsorption process. The data were collected using adsorption study at 298, 318 and 338 K with a resin dosage of 10 mg of resin in 20 ppm Cr(III) (20 mL). A plot of lnK_c versus $1/T$ (**Figure 3.9a**) using Van't Hoff eq (13) in the linear form gave the ΔH^o and ΔS^o values which were used to compute the ΔG^o using eq (14):

$$\ln K_c = \frac{\Delta S^0}{R} - \frac{\Delta H^0}{RT} \quad (14)$$

$$\Delta G^0 = \Delta H^0 - T\Delta S^0 \quad (15)$$

The standard thermodynamic equilibrium constant K_c is equated to q_e/C_e (L/mg) [45, 46]. The decrease in ΔG^0 values (-3.4, -3.8, and -4.3 kJ/mol) with the increase in temperature and their negative sign reveals the adsorption as a favorable process. The positive ΔH^o value of 26 kJ/mol implies endothermic adsorption. The ΔS^o positive value of 5.9 J/mol.K indicates the affinity of the resin towards Cr(III) with an increase in randomness at the solid-solution interface.

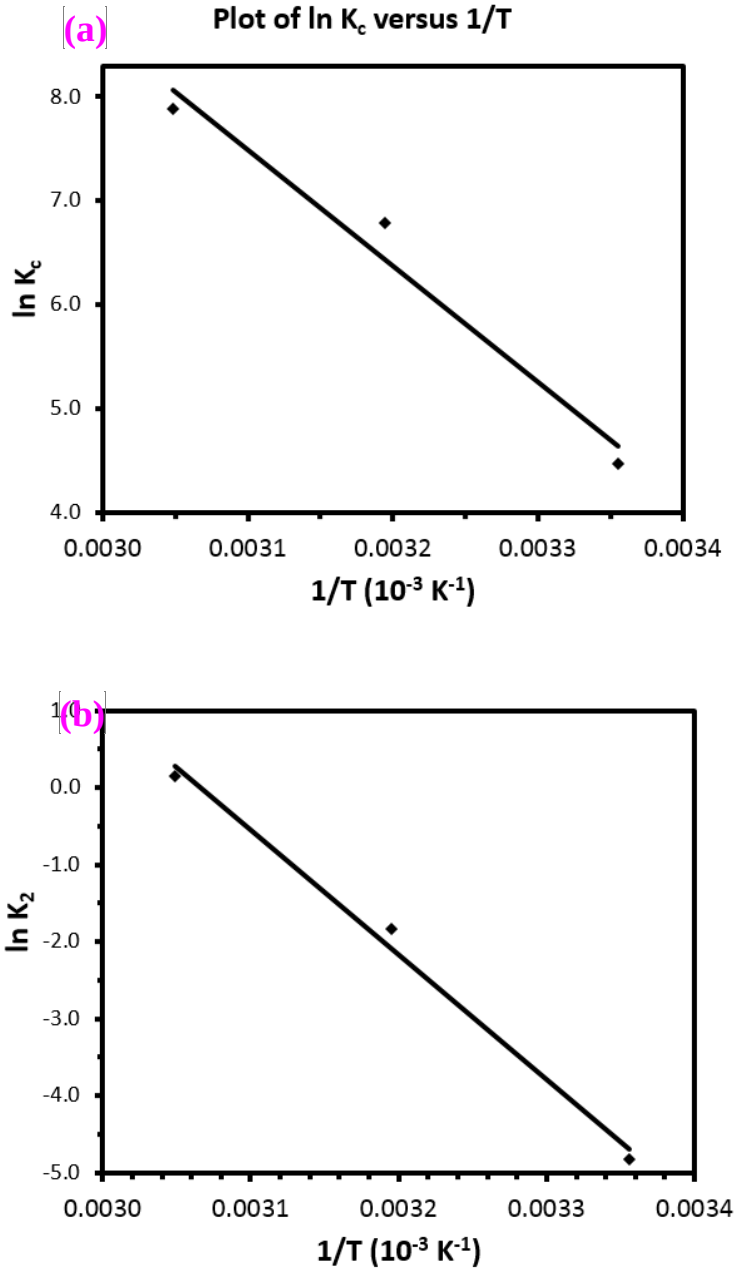

Figure 3.9 (a) Plot of ln Kc versus 1/T and (b) Arrhenius plot of ln k2 versus 1/T for Cr(III) adsorption on the resin [resin dosage of 10 mg in 20 ppm Cr(III) (20 mL)]

3.3.6 Characterization of the spent adsorbent

The resin's surface morphology and structure were evaluated using a scanning electron microscope (SEM), energy dispersive X-ray (EDX) analyses, elemental mapping and FTIR spectroscopy. The analysis of the adsorbate loaded resin was conducted using SEM and EDX. After adsorption, the resin was separated. As depicted in **Figure 3.10**, one can notice the presence of the chromium in the EDX spectrum at 0.6 and 5.4 and 5.9 keV. The chromium mapping gives some indication of the adsorbate distribution on the resin. The data confirm the possible binding of Cr(III) to the surface of the polymer. The low intensity of the Cr peaks in the EDX spectrum could be due to the use of low concentration of Cr(III). The FTIR spectra of resin **4** and Cr(III)-loaded **4** are displayed in **Figure 3.2b.** The shape of the absorption bands of the phosphonate groups at ≈1100 cm^{-1} (**Figure 3.2a**) has been changed in **Figure 3.2b** as a result of bonding with Cr(III) ions, presumably as a result of chelation between the phosphonate groups and the chromium ions. The appearances of a new strong band 1385 cm^{-1} (**Figure 3.2b**) can be assigned to the presence of nitrate ions since chromium nitrate was used in the experiments [46]. Interestingly, the presence of this band indicates the ability of the polymer to act as an anion exchanger [54] in addition to being cationic exchanger. This is due to the presence of charges of both algebraic signs in resin **4** at the pH of 5 (Scheme 1). It is not surprising since the resin has 10 mol% cross-linker having a permanent positive nitrogens of ≈20 mol% that can act as anion exchanger. Appearance of a peak at 540 cm^{-1} is attributed to Cr(III)-O bond formed through oxygen atoms of the phosphonic acid group [46]. The P-O peaks are perturbed in Cr(III)-loaded resin, thereby implying a complex formation between the metal ions and the phosphonate group [54, 55].

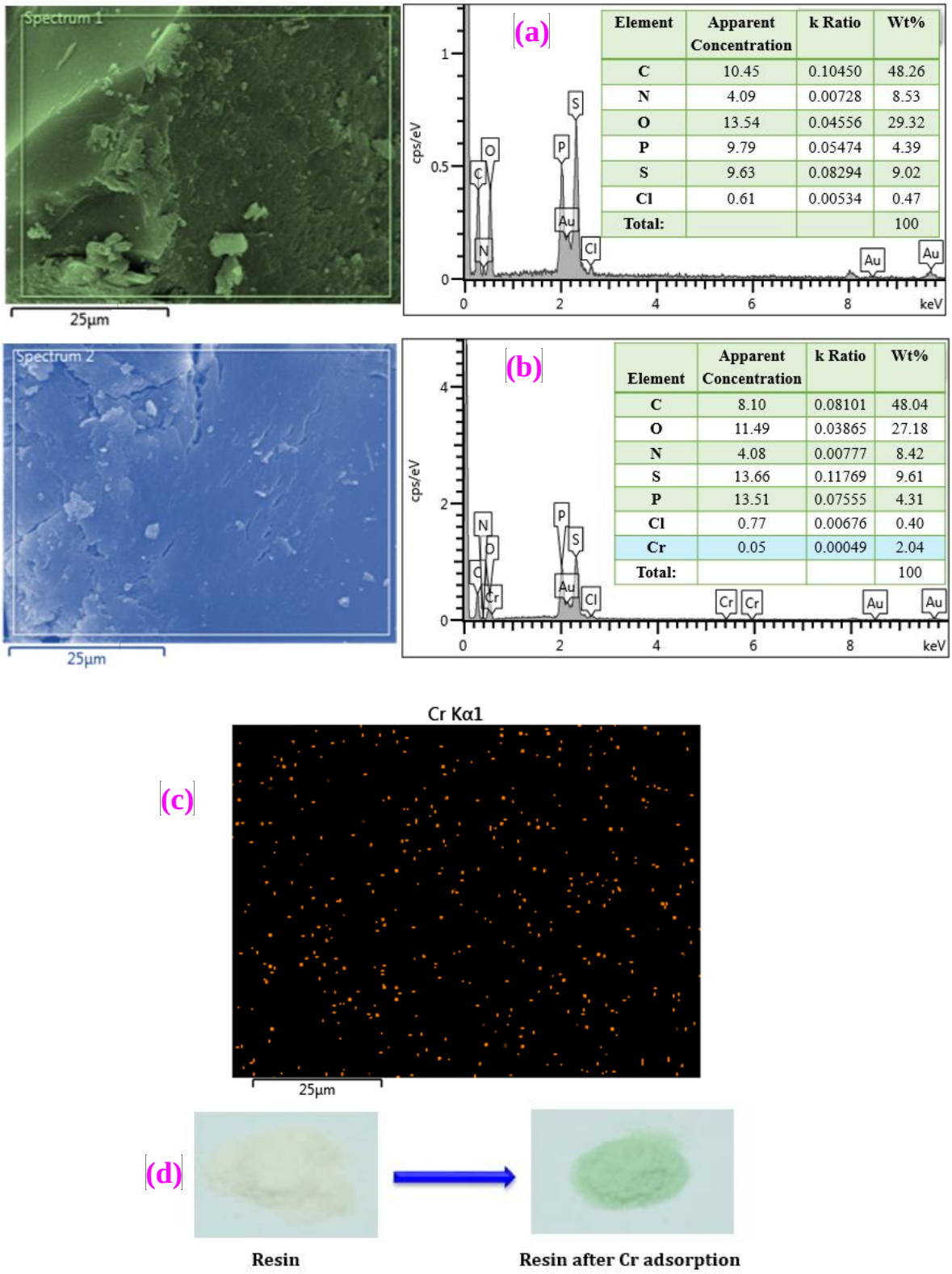

Figure 3.10 SEM images and EDX spectra with a table of analysis of (a) the resin 4, (b) Cr(III)-loaded resin and (c) Chromium elemental mapping of the Cr(III)-loaded resin; (d) photo showing the colour of the resin before and after the Cr adsorption

3.3.7 Individual and simultaneous removal of dyes and metal ions from industrial wastewater

Since the resin was designed with hydrophobic branches that can attract the organic pollutants, it was also evaluated for the removal of various dyes (1 ppm each) in the presence of Cr (III). The resin showed remarkable efficiency in removing methyl orange, Eriochrome black T, rhodamine B, methyl red and methylene blue with efficiencies of ≈100, ≈100, 95, 92, and 90%, respectively, achieved in 30 min, while the results indicated ≈100% removal of Cr(III) as the Cr(III) level in the filtrate was found to be <MDL (i.e. 1 ppb). The changes in the color of the dye solutions before and after mixing with the resin are displayed in **Figure 3.11**.

Thus, the results so far encouraged us to investigate the efficacy of the resin with a real sample. The industrial wastewater samples (pH 6.3) were used to study the effect of the matrix. The sample was spiked with 10000 (μg L^{-1}) Cr(III) and 1 ppm of methyl orange and Eriochrome black T, and then treated with the resin. The dye concentrations were analyzed using the UV-vis spectrophotometer. **Table 3.5** presents the analysis of wastewater sample. The % removals are remarkable; the resin captured efficiently not only the metal ions but also arsenate ions, suggesting its efficiency as an anion exchanger. It is indeed pleasing to see the almost complete simultaneous removal of the dye as well as metal ions.

The regeneration of the used resin was successfully achieved by using 0.1 M HNO_3 at room temperature for 2 h. The polymer has demonstrated remarkable efficiency in removing toxic Cr(III) ions from waters even after 3 cycles with ±4% changes.

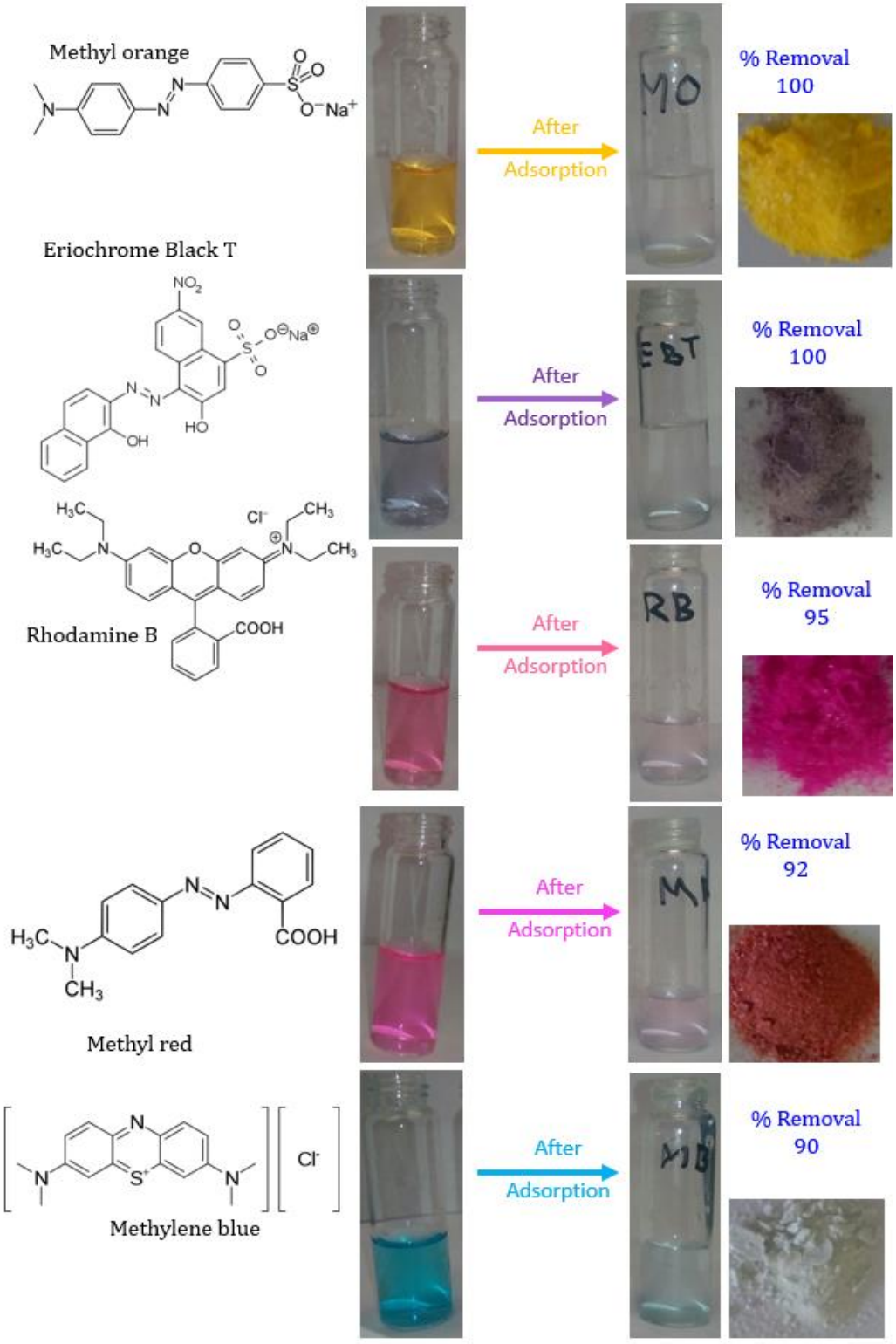

Figure 3.11 Photos showing the change in the color of the dye solutions before and after mixing with the resin and the color of the solid resin after adsorption

Table 3.5 Cr(III) and dye concentrations in wastewater sample before and after the treatment with the resin

Metal	Original sample ($\mu g\ L^{-1}$)	Original sample *spiked* with 10000 ($\mu g\ L^{-1}$) Cr(III) and 1 ppm dyes; then treated with the polymer	Removal (%)
Cr	8.58	76.3	99
Pb	13.28	0.08	96
Cd	2.38	0.013	60
Cu	652.2	258	59
As	4.85	0.92	81
Mo	21.20	1.27	93
Ni	4.31	< MDL	≈100
Methyl orange	1 ppm	< MDL	≈100
Eriochrome black T	1 ppm	< MDL	≈100

MDL: the method detection limit

3.3.8 Reuse of the resin

For economic and environmental reason, recycling and reusability of the resin is an important aspect. As described in the experiment section, the adsorption/desorption experiments were repeated three times. The desorbed samples also demonstrated similar efficiency as the original sample. The resin shows good recovery with almost stable efficiency for the second and third adsorption/desorption cycles. The results of three (3)

cycles of adsorption/desorption procedures are displayed in **Figure 3.12**. The resin has demonstrated remarkable efficiency in removing toxic

Cr(III) ions from waters even after 3 cycles with ± 4% changes. For binary systems, the efficiency remained stable within ± 3-4% for the removal of Cr(III) and Eriochrome Black T.

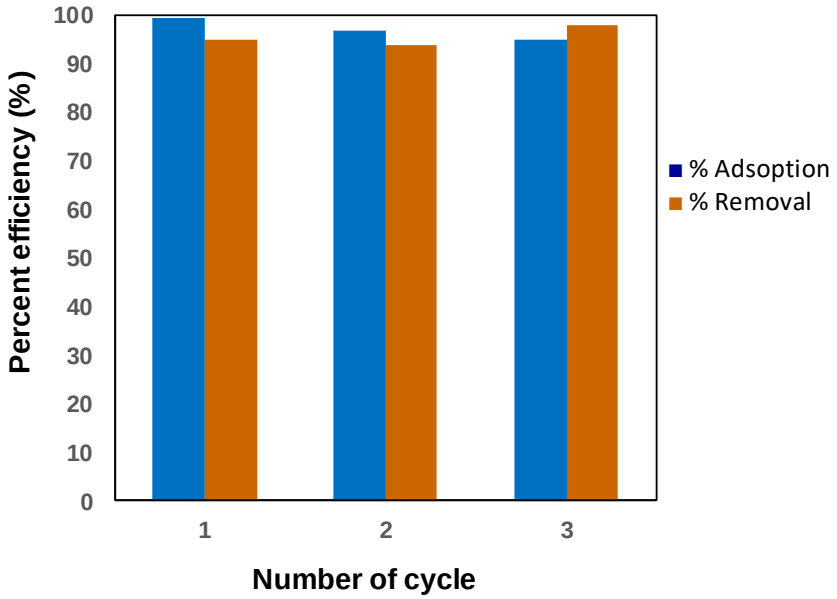

Figure 3.12 Adsorption/desorption with repeated cycles on resin 4

[Experimental conditions: (i) Adsorption: amount of resin: 20 mg, volume of medium: 40 mL, temperature: 298 K, initial concentration of Cr(III): 1.0 ppm, initial pH: 5.0, (ii) Desorption 0.1 M HNO_3].

3.3.9 Immobilization mechanism

The adsorption capacities of Cr(III) is increases with increasing pH values in the range 3.0−7.0. The chelating functionality of aminopropylphosphonate may act as a tridentate ligand as depicted in **B** [56,57] in **Figure 3.13**. While the dye is soluble in water, it can also display hydrophobic interaction because of the organic skeleton. The adsorption of MB, as

well as the other dyes tested, may well be augmented *via* hydrophobic interaction and π–π stacking as depicted in **C** (**Figure 3.13**) [58]. Owing to resonance, the highly dispersed positive charge in MB is expected to have weak ionic/electrostatic interaction with anionic $–PO_3H^-$ motifs in the resin. Note that zwitterionic motifs are prevalent in resin **4**; as such it can exert electrostatic attraction as well as H-bonding interactions to dyes of both algebraic signs The resin/dye interaction is expected to be a physical adsorption process. After washing with acetone, the dye was removed from the dye-loaded resin, and the colored resin returned back to its original color (**Figure 3.11**). The regenerated resin was found to be spectrally (FTIR) similar to the original sample, while the regenerated dye remained stable as evinced by UV-Vis spectroscopic analysis.

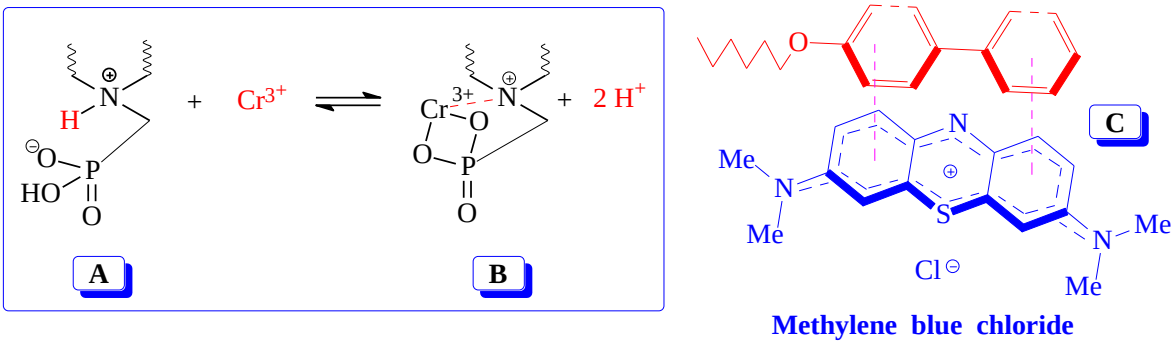

Figure 3.13 Aminopropylphosphonate as a chelating ligand to Cr(III) and stacking methylene blue

3.4 Conclusions

We have reported on the synthesis, chemical, morphological and thermal evaluation of a novel resin. The resin is synthesized using one-step polymerization of monomers **1**, **2** and cross-linker **3**; the monomers are synthesized in excellent yields from readily available starting materials [31-33]. We reported on the investigation of its adsorption potential in simultaneous exclusion of Cr(III) ions and dyes including methyl orange, Eriochrome black T, rhodamine B, methyl red and methylene blue from aqueous media. The resin showed excellent adsorption performance with high Langmuir monolayer capacity at pH 5. The dosage, temperature, and pH, as well as the surface active sites all, contribute to adsorption efficiency. The regeneration tests were achieved efficiently by using 0.1 M HNO_3 for Cr(III). The reported resin is remarkably successful in removing metal ions including arsenic and dyes from industrial wastewater.

3.5 References

[1] L.D. Mafu, T.M. Msagati, B.B. Mamba, Adsorption studies for the simultaneous removal of arsenic and selenium using naturally prepared adsorbent materials, Int. J. Environ. Sci. Technol. 11 (2013) 1723–1732.

[2] D. Mohan, C.U. Pittman, Arsenic removal from water/wastewater using adsorbents-- A critical review, J. Hazard. Mat. 142 (2007) 1–53.

[3] B. Ergül, N. Bektaş, M.S. Öncel, The Use of Manganese Oxide Minerals for the Removal Arsenic and Selenium Anions from Aqueous Solutions, Energ. Environ. Eng. 2 (2014) 103–112.

[4] P. Mondal, C.B. Majumder, B. Mohanty, Laboratory based approaches for arsenic remediation from contaminated water: recent developments, J. Hazard. Mat. 137 (2006) 464–79.

[5] M. Barwick, W. Maher, Biotransference and biomagnification of selenium copper, cadmium, zinc, arsenic and lead in a temperate seagrass ecosystem from Lake Macquarie Estuary, NSW, Australia, Mar. Environ. Res. 56 (2003) 471-502.

[6] T.A. Saleh, Mercury sorption by silica/carbon nanotubes and silica/activated carbon: a comparison study, J. Water Supply Res. T. 64 (2015) 892-903.

[7] H. Saitúa, M. Campderrós, S. Cerutti, A. P. Padilla, Effect of operating conditions in removal of arsenic from water by nanofiltration membrane, Desalination 172 (2005) 173-180.

[8] T.R. Harper, N.W. Kingham, Removal of arsenic from wastewater using chemical precipitation methods, Water Environ. Res. 64 (1992) 200-203.

[9] S. Song, A. Lopez-Valdivieso, D.J. Hernandez-Campos, C. Peng, M.G. Monroy-Fernandez, I. Razo-Soto, Arsenic removal from high-arsenic water by enhanced coagulation with ferric ions and coarse calcite, Water Res. 40 (2006) 364-372.

[10] P. R. Kumar, S. Chaudhari, K.C. Khilar, S.P. Mahajan, Removal of arsenic from water by electrocoagulation, Chemosphere 55 (2004) 1245-1252.

[11] X. Meng, G.P. Korfiatis, C. Christodoulatos, S. Bang, Treatment of arsenic in Bangladesh well water using a household co-precipitation and filtration system, Water Res. 35 (2001) 2805-2810.

[12] T.M. Suzuki, M.L. Tanco, D.A. Pacheco Tanaka, H. Matsunaga, T. Yokoyama, Adsorption characteristics and removal of oxo-anions of arsenic and selenium on the porous polymers loaded with monoclinic hydrous zirconium oxide, Separ. Sci. Technol. 36 (2001) 103-111.

[13] B. Samiey, C.-H. Cheng, J. Wu, Organic-Inorganic Hybrid Polymers as Adsorbents for Removal of Heavy Metal Ions from Solutions: A Review, Materials 7 (2014) 673-726.

[14] G.J. Alaerts, P. Kelderman, Use of coconut shell-based activated carbon for chromium (III) removal, Water Sci Technol. 21 (1989) 1701–1704.

[15] F. Kanwal, M. Imran, L. Mitu, Z. Rashid, H. Razzaq, Q. Ain, Removal of Chromium(III) Using Synthetic Polymers, Copolymers and their Sulfonated Derivatives as Adsorbents, E-Journal of Chemistry, 9 (2012), 621-630.

[16] M. Rafatullah, O. Sulaiman, R. Hashim, A. Ahmad, Adsorption of methylene blue on low-cost adsorbents: a review, J. Hazard. Mater. 177 (2010) 70-80.

[17] P. Liu, L.X. Zhang, Adsorption of dyes from aqueous solutions or suspensions with clay nano-adsorbents, Sep. Purif. Technol, 58 (2007) 32-39.

[18] S. Kabiri, D.N.H. Tran, M. A. Cole, D. Losic, Functionalized three-dimensional (3D) graphene composite for high efficiency removal of mercury, Environ. Sci.:Water Res. Technol. 2 (2016) 390-402.

[19] L.M. Cui, X.Y. Guo, Q. Wei, Y.G. Wang, L. Gao, L.G. Yan, T. Yan, B. Du, Removal of mercury and methylene blue from aqueous solution by xanthate functionalized magnetic graphene oxide: Sorption kinetic and uptake mechanism, J. Colloid Interf. Sci. 439 (2015) 112-120.

[20] A. Mehdinia, M. Akbari, T.B. Kayyal, M. Azad, High-efficient mercury removal from environmental water samples using di-thio grafted on magnetic mesoporous silica nanoparticles, Environ. Sci. Pollut. Res. 22 (2015), 2155-2165.

[21] T.A. Saleh, Isotherm, kinetic, and thermodynamic studies on Hg (II) adsorption from aqueous solution by silica-multiwall carbon nanotubes, Environ. Sci. Pollut. Res. 22 (2015), 16721-16731.

[22] Y.F. Guo, J. Deng, J.Y. Zhu, C. Zhou, C.Y. Zhou, X.J. Zhou, R.B. Bai, Removal of anionic azo dye from water with activated graphene oxide: kinetic, equilibrium and thermodynamic modeling, RSC Adv. 6 (2016), 39762-39773.

[23] T.A. Saleh, A. Sarı, M. Tuzen, Effective adsorption of antimony (III) from aqueous solutions by polyamide-graphene composite as a novel adsorbent, Chem. Eng. J. 307 (2017) 230-238.

[24] B. Henriques, G. Goncalves, N. Emami, E. Pereira, M. Vila, P. Marques, Optimized graphene oxide foam with enhanced performance and high selectivity for mercury removal from water, J. Hazard. Mater. 301 (2016) 453-461.

[25] Y. K. Zhang, T. Yan, L. G. Yan, X.Y. Guo, L.M. Cui, Q. Wei, B. Du, Preparation of novel cobalt ferrite/chitosan grafted with graphene composite as effective adsorbents for mercury ions, J. Mol. Liq. 198 (2014) 381-387.

[26] J.-H. Deng, X. -R. Zhang, G. -M. Zeng, J.-L. Gong, Q.-Y. Niu, J. Liang, Simultaneous removal of Cd(II) and ionic dyes from aqueous solution using magnetic graphene oxide nanocomposite as an adsorbent, Chem. Eng. J. 226, (2013), 189-200.

[27] G. Z. Kyzas, P. I. Siafaka, E. G. Pavlidou, K. J. Chrissafis, D. N. Bikiaris, Synthesis and adsorption application of succinyl-grafted chitosan for the simultaneous removal of zinc and cationic dye from binary hazardous mixtures, Chem. Eng. J. 259 (2015) 438-448.

[28] S.D. Alexandratos, Ion-Exchange Resins: A Retrospective from Industrial and Engineering Chemistry Research, Ind. Eng. Chem. Res. 48 (2009) 388–398.

[29] A. Deepatana, M. Valix, Recovery of nickel and cobalt from organic acid complexes: adsorption mechanisms of metal-organic complexes onto aminophosphonate chelating resin, J. Hazard. Mater. 137 (2006) 925-33.

[30] S.A. Ali, I.W. Kazi, N. Ullah, A New Chelating Ion-Exchange Resin Synthesized via Cyclopolymerization Protocol and its Uptake Performance for Metal Ions Removal, Ind. Eng. Chem. Res. 54 (2015) 9689–9698.

[31] K. Riedelsberger, W. Jaeger, Polymeric aminomethylphosphonic acids-1. Synthesis and properties in solution, Des. Monomers Polym. 1 (1998) 387−407.

[32] S.A. Ali, S. Z. Ahmed, Z. Hamad, Cyclopolymerization studies of diallyl- and tetraallylpiperazinium salts, J. Appl. Polym. Sci. 61 (1996) 1077-1085.

[33] A. Yamaguchi, A. Yoshizawa, Phase Transition Behaviour of amphiphilic supermolecules possessing a semiperfluorinated alkyl chain, Mol. Cryst. Liq. Cryst. 479, 181–189, 2007.

[34] S. Kudaibergenov, W. Jaeger, A. Laschewsky, Polymeric Betaines: Synthesis, Characterization and Application, Adv. Polym. Sci. 201 (2006) 157-224.

[35] G.B. Butler, Cyclopolymerization and cyclocopolymerization, *Marcel Dekker, New York,* 1992.

[36] H. Martínez-Tapia, Synthesis and Structure of $Na_2[(HO_3PCH_2)_3NH]1.5H_2O$: The First Alkaline Triphosphonate, J. Solid State Chem. 151 (2000) 122-129.

[37] V.C.G.D. Santos, Highly improved chromium (III) uptake capacity in modified sugarcane bagasse using different chemical treatments, Quím. Nova. 35 (2012) 1606-1611.

[38] J. Ščančar, Milačič R., A critical overview of Cr speciation analysis based on high performance liquid chromatography and spectrometric techniques, J. Analyt. Atomic Spectrom. 29 (2014) 427-443.

[39] S. Lagergren, About the theory of so-called adsorption of solution substances, K. Sven. Vetenskapsakad. Handl. 24 (1898) 1-39.

[40] Y.S. Ho, G. McKay, Sorption of dye from aqueous solution by peat, Chem. Eng. J. 70 (1998) 115-124.

[41] W.J. Weber Jr., J.C. Morris, Kinetics of adsorption on carbon from solution, J. Sanit. Eng. Div. Proceed. Am. Soc. Civil Eng. 89 (1963) 31–59.

[42] I. Langmuir, The adsorption of gases on plane surfaces of glass, mica and platinum, J. Am. Chem. Soc. 40 (1918) 1362-1403.

[43] T.W. Weber, R. K. Chakravorti, Pore and solid diffusion models for fixed-bed adsorbers, AIChE J. 20 (1974) 228-238.

[44] H.M.F. Freundlich, Over the Adsorption in Solution, J. Physic. Chem. 57, (1906) 385-471.

[45] M.I. Tempkin, V. Pyzhev, Kinetics of ammonia synthesis on promoted iron catalyst, Acta Phys. Chim. USSR, 12 (1940) 327–356.

[46] S. K. Sahni, R. V. Bennekom, J. A. Reedijkhttp://www.sciencedirect.com/science/article/pii/S0277538700872411 -COR1#COR1, A spectral study of transition-metal complexes on a chelating ion-exchange resin containing aminophosphonic acid groups, Polyhedron 4 (1985) 1643-1658.

[47] F.C. Wu, R.L. Tseng, R.S. Juang, Initial behavior of intraparticle diffusion model used in the description of adsorption kinetics, Chem. Eng. J. 153 (2009) 1−8.

[48] S. Kocaoba, G. Akcin, Removal and Recovery of Chromium and Chromium Speciation with MINTEQA2, Talanta 57 (2002) 23-30.

[49] F. Gode and E. Pehlivan, Removal of Chromium (III) from Aqueous Solutions Using Lewatit S 100: The Effect of pH, Time, Metal Concentration and Temperature, J. Hazard. Mater. 136 (2006) 330-337.

[50] S. Kocaoba and G. Akcin, Removal of Chromium(III) and Cadmium(II) from Aqueous Solutions, Desalination 180 (2005) 151-156.

[51] S. Kocaoba and G. Akcin, Removal and Recovery of Chromium and Chromium Speciation with MINTEQA2, Talanta 57 (2002) 23-30.

[52] G.J. Alaerts, V. Jitjaturunt, P. Kelderman Use of coconut shell-based activated carbon for chromium(VI) removal, Water Sci. Technol. 21 (1989) 1701-1704.

[53] F. Kanwal, M. Imran, L. Mitu, Z. Rashid, H. Razzaq , Q. Ain, Removal of Chromium(III) Using Synthetic Polymers, Copolymers and their Sulfonated Derivatives as Adsorbents, E-Journal of Chemistry 9 (2012) 621-630.

[54] D. Kolodynska, Z. Hubicki and S. Pasieczna-Patkowska, FT-IR/PAS Studies of Cu(II)–EDTA Complexes Sorption on the Chelating Ion Exchangers, Acta Phys. Pol. A 116 (2009) 340–343.

[55] J. Sheals, P. Persson and B. Hedman, IR and EXAFS Spectroscopic studies of glyphosate protonation and copper(II) complexes of glyphosate in aqueous solution, Inorg. Chem. 40 (2001) 4302-4309.

[56] D. Kołodynska, Z. Hubicki, M. Geca, Application of a New-Generation Complexing Agent in Removal of Heavy Metal Ions from Aqueous Solutions, Ind. Eng. Chem. Res. 47 (2008) 3192-3199.

[57] T.A. Saleh, A.M. Muhammad, S.A. Ali, Synthesis of hydrophobic cross-linked polyzwitterionic acid for simultaneous sorption of Eriochrome black T and chromium ions from binary hazardous waters, J. colloid interf. Sci. 468 (2016) 324-333.

[58] X. He, K.B. Male, P.N. Nesterenko, D. Brabazon, B. Paull, and J.H.T. Luong, Adsorption and Desorption of Methylene Blue on Porous Carbon Monoliths and Nanocrystalline Cellulose, ACS Appl. Mater. Interfaces 5 (2013) 8796–8804.

CHAPTER 4

CONCLUSION AND RECOMENDATION

The present study was focused on the synthesis, chemical, morphological and thermal characterization of a new novel polymer. We reported on the investigation of adsorption potential of newly developed polymer in the single and simultaneous exclusion of Hg(II) ions and methylene blue from aqueous solutions. The resin showed good adsorption performance with high Langmuir monolayer adsorption capacity at pH 5 at 24 °C. The kinetic assessments revealed that the adsorption process of Hg(II) and methylene blue onto the polymer was progressed via the second-order kinetic mechanism with an R^2 value of >0.99 for all studied concentrations. The initial concentration, temperature, and pH as well as the surface-active sites all contribute to adsorption efficiency. The regeneration tests were achieved by using 0.1 M HCl for Hg(II) and acetone for methylene blue. In addition to being cost-effective, the resin has advantageous properties such as active sites, high adsorption capacity, high reusability, easy-to-use, and cost-effective. The polymer has demonstrated remarkable efficiency in simultaneous removal of toxic Hg(II) ions and methylene blue from aqueous systems.

We have reported on the synthesis, chemical, morphological and thermal evaluation of a novel polymer. We reported on the investigation of adsorption potential of newly developed polymer in the single and simultaneous exclusion of Cr(III) ions and dyes including methyl orange, Eriochrome black T, rhodamine B, methyl red and methylene blue from aqueous media. The resin showed good adsorption performance with high Langmuir monolayer adsorption capacity at pH 5 at room temperature. The kinetic assessments revealed removal of Cr(III) and methylene blue onto the polymer was progressed via the second-order kinetic

mechanism with high R^2 value. The dosage, temperature, and pH, as well as the surface active sites all, contribute to adsorption efficiency. The regeneration tests were achieved by using 0.1 M HNO_3 for Cr(III). The reported resin is very promising for real applications due to its advantageous properties such as active sites, high adsorption capacity, high reusability, easy-to-use, and cost-effective.

VITAE

Name	:Ihsan Budi Rachman
Nationality	:Indonesia
Date of Birth	:2/13/1989
Email	:ihsanbudir@gmail.com
Address	:Jl. Kyai Ahmad Fadlil II No. 19 Ciamis Jawa Barat Indonesia
Academic Background	: Bachelor degree in Chemistry from Institut Teknologi Bandung, West Java, Indonesia in July 2013 : Master degree in Chemistry from King Fahd University of Petroleum and Minerals, Dhahran, Saudi Arabia in May 2017

List of Publications :

1. TA Saleh, IB Rachman, SA Ali, Tailoring hydrophobic branch in polyzwitterionic resin for simultaneous capturing of Hg(II) and methylene blue with response surface optimization, **Nature Scientific Reports** 7, 4573. Doi 10.1038/s41598-017-04624
2. SA Ali, IB Rachman, TA Saleh, Simultaneous trapping of Cr(III) and organic dyes by a pHresponsive resin containing zwitterionic aminomethylphosphonate ligans and hydrophobic pendants, **Chemical Engineering Journal** 330, 663 – 674. Doi 10.1016/j.cej.2017.08.003
3. IB Rachman, D Wahyuningrum, Synthesized 2,4,5-Triphenylimidazole as precursor of organic light emitting diode material, **Advanced Material Research** 896, 468 – 471. Doi 10.4028/www.scientific.net/AMR.896.468